

A new matheuristic and improved instance generation for kidney exchange programmes

Maxence Delorme[‡], Sergio García^{*}, Jacek Gondzio^{*}, Joerg Kalcsics^{*}, David Manlove[†],
William Pettersson^{*†}, and James Trimble[†]

[‡]*Department of Econometrics and Operations Research, Tilburg University, The Netherlands*

[†]*School of Computing Science, University of Glasgow, United Kingdom*

^{*}*School of Mathematics, University of Edinburgh, United Kingdom*

June 2, 2021

Abstract

Kidney exchange programmes increase the rate of living donor kidney transplants, and operations research techniques are vital to such programmes. These techniques, as well as changes to policy regarding kidney exchange programmes, are often tested using random instances created by a Saidman generator. We devise a new matheuristic that can optimally solve a benchmark set of Saidman instances in seconds: these instances have not been solved in under thirty minutes previously. This is possible as we take advantage of particular properties of these random instances that are noticeably different in real-world instances. We follow up this matheuristic with new techniques for generating random kidney exchange instances that are far more similar to real-world instances from the UK kidney exchange programme. This new process for generating random instances provides a more accurate base for comparisons of algorithms and models, and gives policy-makers a better understanding of potential changes to policy leading to an improved decision-making process.

1 Introduction

1.1 Background

Kidney disease affects millions of people worldwide, and the two known treatment options for end-stage kidney disease are dialysis and kidney transplantation. Of these options, kidney transplantation offers a better quality of life, better life expectancy, and is cheaper [6], but donor kidneys are in short supply. These kidneys are donated by either deceased or living donors, with better outcomes for the recipient correlated with living donors [18, 32]. However, it is difficult for a recipient to find a compatible and willing living donor on their own. A Kidney Exchange Programme (KEP) alleviates the need for recipients to be compatible with their own donors [28]. Instead, recipients join KEPs with a willing paired donor (or multiple willing paired donors), and at certain times the KEP performs a matching run, determining an optimal set of exchanges to perform such that a donor donates a kidney if their paired recipient receives a kidney (and at most one donor paired with any recipient donates a kidney). These exchanges involving recipients with paired donors form cycles: the length of these cycles is often limited for logistical reasons, but limiting this maximum length can reduce the efficiency of a KEP. Additionally, individuals can join a KEP to donate a kidney without expecting any reciprocal donation: such individuals are referred to as non-directed (or altruistic) donors, and donors paired with a recipient are called directed donors. Non-directed donors can initiate a chain of transplants, by donating to a recipient whose donor can then donate to a further recipient and so-on. We will use the term exchange to refer to either a cycle or a chain.

*william.pettersson@glasgow.ac.uk, Corresponding author

41 Identifying the potential transplants is a vital part of the operation of a KEP, and numerous operations
42 research techniques and algorithms have been devised for finding such exchanges. The problem of
43 finding a largest set of transplants is polynomial-time solvable in very restricted settings (such as limiting
44 cycle and chain lengths to 2), but in general is NP-hard [1], and so integer programming (IP) is often
45 used to find solutions. The first IP models used one variable for either each potential cycle [29] or
46 each edge [1], but there have been numerous substantial improvements in this area, including compact
47 formulations as well as column generation, branch-and-price, branch-and-price-and-cut, and failure-aware
48 modelling [2, 3, 12, 13, 14, 21, 23, 25]. A summary of models and techniques currently in use by real-world
49 KEPs is also available [9].

50 In this paper we use the UK Living Kidney Sharing Scheme (UKLKSS) as our real-world KEP
51 example [23]. The UKLKSS is run by NHS Blood and Transplant, a special health authority of the
52 National Health Service (NHS) within UK. The UKLKSS has been operating since 2007, and is currently
53 the largest KEP (by both pool size and transplant count) in Europe [8].

54 We use the term *Kidney Exchange problem* (KE) to refer to the problem of finding a set of cycles
55 and chains that yield the maximum number of transplants, given a dataset containing information
56 about donors, recipients and compatibilities between them. The effectiveness of the techniques used to
57 find optimal sets of exchanges is often compared using randomly-generated instances that are created
58 to mimic real-world instances. Such random instances are also useful for policy-makers, as they allow
59 changes to policies (such as prioritisation of highly-sensitised patients, or the introduction of a wider range
60 of exchange structures) to be tested. In the literature, a generator due to Saidman et al., henceforth
61 referred to as the *Saidman generator*, is commonly used to generate such instances [30]. The Saidman
62 generator draws recipients and donors with various properties (such as blood-groups) based on the
63 random distribution of such parameters in populations. A more thorough introduction to the Saidman
64 generator is given in Section 5.2. We also highlight that PrefLib [24], an online repository of matching
65 problems with preferences, includes a set of instances that have been generated using the Saidman
66 generator [14]. We will refer to these as the PrefLib instances. The best known result in the literature
67 for these particular instances has been demonstrated by Lam and Mak-Hau [21], who use a branch-and-
68 price-and-cut algorithm to solve all 30 non-trivial instances when cycles are limited to length 3, and 19
69 of 30 non-trivial instances when cycles are limited to length 4. However, these PrefLib instances differ
70 from real-world instances in a range of parameters (such as edge density), meaning that algorithms that
71 can solve the PrefLib instances quickly may not be as applicable to real-world problems and vice-versa.

72 1.2 Related work

73 Many different approaches to improving the performance of KEPs have been investigated in the literature.
74 We outline here two particular developments in the field, and highlight that for both of these, and indeed
75 for almost any improvement to KEPs, the simulation of any proposed changes depends on the use of
76 suitable random or benchmark instances for a baseline comparison.

77 The creation of transnational KEPs, either as new programmes or through coordination between
78 or amalgamation of existing national programmes, allows KEPs to share their pools, thus increasing
79 their overall effectiveness through more efficient allocation of resources. However, collaboration between
80 countries when human organs are involved is a sensitive issue, both ethically and legally. Individual
81 rationality has been proposed as one requirement for such collaboration [4, 5], and further research has
82 suggested equality measures such as the Shapley value [7] as well as IP models that allow for, and have
83 simulated, different constraints within different countries [26]. We note that KEPs within some countries
84 (such as the USA) may exhibit similar characteristics without being transnational, as transplant centres
85 (or groups of transplant centres) either collaborate or compete for kidney transplants [22].

86 Another important development in the field of kidney exchange is the introduction of robust, or fault-
87 tolerant, KEPs. A potential transplant may be selected by an algorithm or policy for transplantation,
88 but may fail due to any one of a number of reasons (e.g., donor or recipient illness, unexpected incom-
89 patibilities). Robust KEP algorithms aim to assign a likelihood of progression (alternatively, a likelihood
90 of failure) to each potential transplant, and then select a set of exchanges that maximises the expected
91 number of transplants. The difficulty of determining the likelihood of whether a potential transplant
92 will proceed in practice is well known, and depends on cPRA (calculated Panel Reactive Antibodies,
93 a score between zero and one hundred assigned to a recipient indicating the likelihood that a random
94 blood-group compatible donor will be tissue-type incompatible, see Section 2.1 for more background),

95 but cannot be explained by cPRA alone [16]. Section 5 in this paper provides a number of new insights
96 into this relationship between cPRA and transplant compatibility. Recent models for KEPs have as-
97 signed a success probability to each potential transplant, and used these to find a set of exchanges that
98 maximises the number of expected transplants [14], and further work has also included various recourse
99 options that model fall-back strategies which may be used when transplants cannot proceed [11, 19].

100 1.3 Our contribution

101 We develop three upper bounds for the potential number of transplants in KE instances by utilising the
102 available blood-group information of donors and recipients. We introduce a new ad-hoc matheuristic
103 that aims to find a solution whose value matches one of the upper bounds. This is possible for every
104 PrefLib instance, which allows us to empirically observe that our matheuristic is significantly faster than
105 known techniques. However for real-world instances used in our experiments, the solution found by
106 the matheuristic does not attain the upper bound, meaning that it does not provide a guarantee of
107 optimality, as is usually required in a KEP.

108 We then study the reasons why real-world instances differ from the PrefLib instances (and more
109 generally, from any instance created by a Saidman generator) highlighting distinctions relative to a
110 number of relevant parameters including edge density and maximum number of potential transplants.
111 We then devise new methods for generating random KE instances, based on the Saidman generator but
112 incorporating improvements that can be justified both statistically and by real-world scenarios. These
113 improvements all involve the calculated Panel Reactive Antibody value (cPRA) of a recipient, which
114 estimates what proportion of donors in the KEP will be tissue-type incompatible with that recipient.
115 The improvements arise from examining:

- 116 • the distribution of cPRA amongst recipients when grouping recipients by their blood-group and
117 the blood-group of their donor,
- 118 • the relationship between cPRA and transplant compatibility, and
- 119 • the transplant compatibility of recipients with a cPRA of zero.

120 We show that our improved generator creates random KE instances that more closely match real-world
121 instances from the UK than the traditional Saidman generator across a wide variety of relevant param-
122 eters.

123 The paper is organised as follows. Section 2 gives a background on and defines terminology and
124 notation used in kidney exchange programmes. Section 3 details our new upper bound methods for the
125 PrefLib instances, while Section 4 introduces our new matheuristic and demonstrates its computational
126 performance on the PrefLib instances. Section 5 then introduces our new techniques for generating
127 random KE instances, and we close with a conclusion in Section 6.

128 2 Background

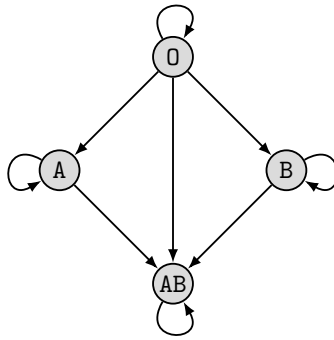
129 We present background on compatibility in KEPs in Section 2.1, and then in Section 2.2 we introduce
130 representations of KE instances as well as terminology used to describe particular structures within such
131 instances.

132 2.1 Compatibility

133 The compatibility of a transplant between a donor and a recipient is determined by a number of different
134 factors. We will describe two in detail as they are relevant to our work, and briefly mention some others.

135 Possibly the most well-known factor is blood-group (or ABO) compatibility. A donor with blood-
136 group O (also called universal donor) can potentially give their kidney to a recipient with any blood-
137 group. A donor with blood-group A (respectively B) can potentially give their kidney to a recipient with
138 blood-group A or AB (respectively B or AB). An AB donor can only give their kidney to an AB recipient
139 (also called universal receiver). This compatibility is often presented as a graph such as Figure 1

Figure 1: Blood-group compatibility



140 Another factor for compatibility is tissue-type compatibility, determined by the presence of human
 141 leukocyte antigens (HLA) in a donor and potential presence of HLA antibodies in a recipient. As
 142 such, this is also known as HLA compatibility. Tissue-type compatibility is best determined with a
 143 lab-based crossmatch test, in which samples from a donor and recipient are combined and examined
 144 for reactions [27]. However, such tests are expensive and time-consuming, so it is often not feasible to
 145 test every single donor against every single recipient. Instead, some alternatives have been developed.
 146 A Panel Reactive Antibody (PRA) test determines a recipient’s PRA value by performing crossmatch
 147 tests against a given panel of samples. The resulting PRA value of a recipient gives the proportion of
 148 donors that a recipient is likely to be incompatible with as a percentage (e.g., a recipient with a PRA
 149 of 0 is likely to be tissue-type compatible with all donors, while a recipient with a PRA of 95 is likely
 150 to be tissue-type compatible with only 5% of donors). A better understanding of HLA incompatibility
 151 has allowed for the testing of the presence or absence of individual antigens or antibodies, resulting in
 152 the calculated PRA (cPRA) parameter. This is calculated based on not only the presence of antigens
 153 in recipients and antibodies in donors, but also a better understanding of which specific antigen and
 154 antibody combinations are more likely to result in a failed transplant. Again, the actual cPRA value for
 155 a recipient aims to represent the proportion of donors with which the recipient will not be compatible
 156 with.

157 Many other factors influence compatibility, including but not limited to, the ages and general health
 158 of the donor and the recipient, the size of the donor kidney, and even potentially the number of veins or
 159 arteries present on the donor kidney.

160 2.2 Notation and terminology

161 We formally define a Kidney Exchange problem (KE) instance as a directed graph $\mathcal{G} = (\mathcal{V}, \mathcal{A})$ (also called
 162 compatibility graph) in which vertex set \mathcal{V} contains every recipient and arc set $\mathcal{A} = \{(i, j) : i, j \in \mathcal{V}\}$
 163 contains the potential transplants: (i, j) belongs to \mathcal{A} if the donor associated to recipient i is compatible
 164 with recipient j . Note that compatible recipient/donor pairs (represented by an arc $(i, i) \in \mathcal{A}$) are
 165 allowed in some KEPs. A feasible *exchange* is a cycle in the directed graph: a sequence of distinct
 166 vertices (v_1, \dots, v_k) such that there is an arc (v_i, v_{i+1}) for each $i \in \{1, \dots, k-1\}$, and an arc (v_k, v_1) .
 167 In an exchange, a donor paired with a recipient only donates a kidney if their paired recipient receives a
 168 kidney. For logistical purposes, there is often an upper bound on how many vertices can be part of any
 169 exchange (named L in the following).

170 Some KEPs also include non-directed donors (sometimes referred to as altruistic donors) who are
 171 willing to donate a kidney without being paired with a recipient. In the compatibility graph, non-
 172 directed donors are represented by a node in \mathcal{V} with no incoming arcs and one outgoing arc to each of
 173 the recipients they are compatible with. In the presence of non-directed donors, an exchange can also be
 174 a *chain*, which is a sequence of distinct vertices (v_1, \dots, v_k) where v_1 corresponds to a non-directed donor,
 175 and for each $i \in \{1, \dots, k-1\}$ there is an arc (v_i, v_{i+1}) . Usually, the donor associated to recipient v_k
 176 gives a kidney to a deceased-donor waiting list.

177 Some KEPs also allow a recipient to be paired with multiple donors. In Sections 3 and 4, we focus
 178 on the PrefLib instances, in which: (i) every recipient is paired with exactly one donor and every donor
 179 is paired with exactly one recipient, (ii) there are no compatible recipient/donor pairs (i.e., no arcs

180 $(i, i) \in \mathcal{A}$), and (iii) there are no non-directed donors. In Section 5 we explicitly allow recipients to be
 181 paired with multiple donors, which more closely matches the real-world instances from the UKLKSS.

182 3 Upper bounds for PrefLib instances

183 In this section, we describe three upper bounding procedures for KE instances with no non-directed
 184 donors. The first bound U_1 , which is valid for any instance, is derived from a relaxation of the cycle size
 185 limit constraints and can be computed in polynomial time. The two other bounds U_2 and U_3 use the
 186 donor and recipient blood-groups to identify a subset of recipient/donor pairs that cannot participate in
 187 a maximum-size exchange, and perform particularly well on PrefLib instances.

188 3.1 Unbounded cycle lengths upper bound

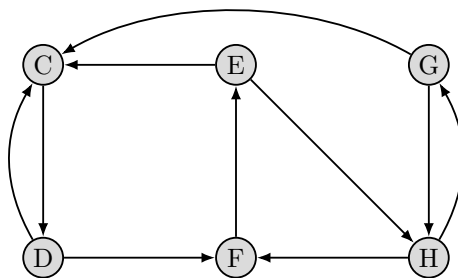
189 It is well known that determining the maximum number of transplants in a kidney exchange instance for
 190 general values of L is \mathcal{NP} -hard. Abraham et al. [1] outlined two cases where the problem can be solved
 191 in polynomial time:

- 192 • When $L = 2$, the compatibility graph can be transformed into an undirected graph $\mathcal{G}' = (\mathcal{V}', \mathcal{E}')$ in
 193 which edge $\{i, j\}$ belongs to \mathcal{E}' if and only if both arcs (i, j) and (j, i) belong to \mathcal{A} in the original
 194 graph. The problem now is to find a matching of maximum size and this can be done in polynomial
 195 time using Edmonds' algorithm [15].
- 196 • When $L = \infty$, the compatibility graph can be transformed into a bipartite graph $\mathcal{G}'' = (\{\mathcal{L}'', \mathcal{R}''\}, \mathcal{E}'')$
 197 where \mathcal{L}'' is the set of donors and \mathcal{R}'' is the set of recipients. There is an edge $\{i, j\}$ in \mathcal{E}'' with
 198 cost 1 if donor i is compatible with recipient j and an edge $\{i, j\}$ in \mathcal{E}'' with cost 0 if i and j are in
 199 the same recipient/donor pair. The problem now is to find a perfect matching of maximum weight,
 200 and again, this can be done in polynomial time using the Hungarian algorithm [20].

201 For a given kidney exchange instance with cycle size limit L , the maximum number of transplants
 202 cannot decrease as L increases. As a result, solving the problem with $L = \infty$ gives an upper bound
 203 on the maximum number of pairs selected in an exchange for any value of $L \in \mathbb{Z}$. We call this upper
 204 bound U_1 .

205 **Example 1.** Let us consider the following kidney exchange instance with 6 recipients and the following
 206 compatibility graph:

Figure 2: Compatibility graph for Example 1



- 207 • If $L \geq 6$, an optimal solution will match the six recipient/donor pairs in either one or two cycles:
 208 $\{[G, C, D, F, E, H]\}$ or $\{[C, D, F, E], [H, G]\}$;
- 209 • If $L = 4$ or 5 , an optimal solution will match the six recipient/donor pairs in two cycles: $[C, D, F, E]$
 210 and $[H, G]$;
- 211 • If $L = 3$, an optimal solution will match five recipient/donor pairs in two cycles: $[E, H, F]$ and
 212 $[D, C]$;
- 213 • If $L = 2$, an optimal solution will match four recipient/donor pairs in two cycles: $[H, G]$ and
 214 $[D, C]$.

215 3.2 Data-driven upper bound

216 Our second upper bound U_2 uses blood-group compatibility (see Section 2) to calculate the maximum
 217 number of transplants that can possibly take place. Note that blood-group compatibility is a necessary
 218 but not sufficient condition for transplant compatibility. In the following, we call:

- 219 • A $*/*$ pair a recipient/donor pair in which the recipient and the donor have any blood group, and
 220 we denote by n the number of $*/*$ pairs.
- 221 • An $X/*$ pair a recipient/donor pair in which the recipient has blood-group X and the donor has any
 222 blood group, and we denote by $n_{X/*}$ the number of $X/*$ pairs.
- 223 • A $*/Y$ pair a recipient/donor pair in which the recipient has any blood-group, and the donor has
 224 blood-group Y and we denote by $n_{*/Y}$ the number of $*/Y$ pairs.
- 225 • An X/Y pair a recipient/donor pair in which the recipient has blood-group X and the donor has
 226 blood group Y , and we denote by $n_{X/Y}$ the number of X/Y pairs.

227 Upper bound U_2 makes the initial assumption that each of the recipient/donor pairs will participate in
 228 the exchange unless stated otherwise. It then uses the two following rules to adjust its value:

- 229 • Since only cycles are allowed, if an $O/*$ pair p cannot be matched with any $*/O$ pair, then p cannot
 230 participate in the exchange.
- 231 • Similarly, if a $*/AB$ pair p cannot be matched with any $AB/*$ pair then p cannot participate in the
 232 exchange.

233 Even though it might be difficult to detect with precision which $O/*$ and which $*/AB$ pairs will be excluded
 234 from the matching, we know that if $n_{O/*} > n_{*/O}$ (i.e., if there are more $O/*$ than $*/O$ pairs), then at least
 235 $n_{O/*} - n_{*/O}$ pairs cannot participate in the exchange. Similarly, we know that if $n_{*/AB} > n_{AB/*}$, then at least
 236 $n_{*/AB} - n_{AB/*}$ pairs cannot participate in the exchange. If we now define $\ell_1 = \max\{0, n_{O/*} - n_{*/O}\}$ as the
 237 minimum number of $O/*$ pairs that cannot participate in the exchange and $\ell_2 = \max\{0, n_{*/AB} - n_{AB/*}\}$
 238 as the minimum number of $*/AB$ pairs that cannot participate in the exchange, then we can formally
 239 introduce the bound $U_2 = n - \ell_1 - \ell_2 + \min\{n_{O/AB}, \ell_1, \ell_2\}$, where the last term identifies the number of
 240 O/AB pairs that were counted both in ℓ_1 and in ℓ_2 . Note that a solution with value U_2 is only reachable
 241 if the following assumptions are met: (i) if $\ell_1 > 0$ (which is the case for every PrefLib instance), then
 242 every O donor is matched with an O recipient (otherwise more than ℓ_1 pairs of the form $O/*$ would not be
 243 able to participate in the exchange), and (ii) if $n_{O/AB}$ is less than or equal to both ℓ_1 and ℓ_2 (which is also
 244 the case for every PrefLib instance), then no O/AB pairs should participate in the exchange (otherwise,
 245 such a pair should be counted both in ℓ_1 and in ℓ_2). These assumptions will be used henceforth.

246 **Example 2.** Let us consider the kidney exchange instance from the PrefLib repository “MD-00001-
 247 00000191”, an instance with $n = 512$ and the following blood-group distribution:

Table 1: Blood-group distribution for Example 2

Rec. / Don.	./O	./A	./B	./AB	./*
O/.	66	134	70	13	283
A/.	51	34	59	11	155
B/.	10	53	4	1	68
AB/.	3	1	1	1	6
*/.	130	222	134	26	512

248 Out of the 512 recipient/donor pairs, we know that 153 ($\ell_1 = 283 - 130$) $O/*$ pairs cannot participate
 249 in the matching because there are not enough $*/O$ pairs to accommodate them. We also know that 20
 250 ($\ell_2 = 26 - 6$) $*/AB$ pairs cannot participate in the matching because there are not enough $AB/*$ pairs
 251 to accommodate them. Out of the 173 removed pairs, we know that up to 13 O/AB pairs could have
 252 potentially been counted twice (i.e., both in ℓ_1 and ℓ_2). This gives an upper bound U_1 equal to 352 (512
 253 - 153 - 20 + 13). An optimal solution to this instance has size 351 if $L = 3$, and size 352 if $L \geq 4$,
 254 showing that, for this particular instance, the bound is very close to the optimal solution value.

3.3 ILP-based upper bound

After some preliminary analysis, we found that the difference observed between upper bounds U_2 and the optimal solutions of the tested PrefLib instances always came from some $*/AB$ pairs that we assumed could be part of the exchange while in reality they could not (in other words, we underestimated ℓ_2). This can be explained by the fact that AB is the least common blood-group, so there are fewer opportunities to match $*/AB$ pairs with $AB/*$ pairs. In order to correct the wrong assumptions, we designed a tailored ILP model that maximises the number of X/AB pairs that can possibly be included in the exchange ($X \in \{A, B, AB\}$) to determine a refined upper bound U_3 . Note that the other assumptions derived from U_2 , namely (i) that any $*/O$ pair must be followed by an $O/*$ pair in the exchange, and (ii) that no O/AB pairs should be included in the exchange, still hold. Every time one of these two assumptions is violated, the exchange size is reduced by one unit. In the following, we first describe the ILP model details for $L = 3$ and then we explain how to modify it for $L = 4$. The model needs a list of every cycle solely composed of $*/AB$ pairs. We distinguish:

- C_2^2 , the set of 2-cycles with two $*/AB$ pairs – these can only be in the form $[AB/AB - AB/AB]$.
- C_3^3 , the set of 3-cycles with three $*/AB$ pairs – these can only be in the form $[AB/AB - AB/AB - AB/AB]$.

For instance, if all the pairs in Example 1 were AB/AB pairs, then there would be two cycles in C_2^2 : $[C, D]$ and $[G, H]$, and one cycle in C_3^3 : $[E, H, F]$. The model also needs a list of every cycle partly composed of $*/AB$ pairs. We distinguish:

- P_2^1 , is the set of *partial* cycles comprising two pairs, among which exactly one is a $*/AB$ pair – these are in the form $[X/AB - AB/Y]$, where $X \in \{A, B, AB\}$ and $Y \in \{O, A, B\}$. These cycles do not necessarily need to be complete, so we make sure that either the donor of the second pair is compatible with the recipient of the first pair, or that there exists at least one additional pair that can complete the cycle;
- C_3^2 , the set of 3-cycles with exactly two $*/AB$ pairs – these are in the form $[X/AB - AB/AB - AB/Y]$, where $X \in \{A, B, AB\}$ and $Y \in \{A, B\}$;

By introducing binary decision variables x_c taking value 1 if cycle c is selected and 0 otherwise ($c \in \mathcal{C}$, where $\mathcal{C} = \{C_2^2 \cup C_3^3 \cup P_2^1 \cup C_3^2\}$), the maximum number of X/AB pairs that can possibly be included in the exchange ($X \in \{A, B, AB\}$) denoted as z can be obtained through the following ILP model:

$$\max \quad z = \sum_{c \in C_2^2} 2x_c + \sum_{c \in C_3^3} 3x_c + \sum_{c \in P_2^1} x_c + \sum_{c \in C_3^2} 2x_c \quad (1)$$

$$\text{s.t.} \quad \sum_{c \in \mathcal{C}: i \in V(c)} x_c \leq 1, \quad \forall i \in \mathcal{V}, \quad (2)$$

$$x_c \in \{0, 1\}, \quad c \in \mathcal{C}, \quad (3)$$

where $V(c)$ indicates the set of recipient/donor pairs that belong to cycle c . Upper bound U_3 can be defined as $U_3 = n - \ell_1 - \ell'_2$ where $\ell'_2 = (n_{*/AB} - z)$. Note that it is not necessary to consider cycles $[O/AB - AB/Y]$ in P_2^1 because selecting such cycle would increase z (and thus, U_3) by one unit at best, but would also break one of our assumptions, decreasing by one unit the exchange size. Similarly, it is not necessary to consider cycles $[O/AB - AB/AB - AB/O]$ in C_3^2 because selecting such cycle would only increase U_3 by one unit (two units in z with a one unit penalty due to the broken assumption), which is as effective as selecting the truncated $[AB/AB - AB/O]$ cycle that already exists in P_2^1 .

The model can be extended to take into account a cycle size limit of four. In this case, we need:

- An additional set of cycles C_4^4 with four $*/AB$ pairs – these can only be in the form $[AB/AB - AB/AB - AB/AB - AB/AB]$.
- An updated set of partial cycles P_2^1 with two pairs having exactly one $*/AB$ pair in which we additionally make sure that either the donor of the second pair is compatible with the recipient of the first pair, or that there exists at least one pair or a couple of pairs that can complete the cycle.

- An updated set of partial cycles P_3^2 with three pairs having exactly two */AB pair – these are in the form $[X/AB - AB/AB - AB/Y]$ where $X \in \{A, B, AB\}$ and $Y \in \{O, A, B\}$. These cycles do not necessarily need to be complete, so we make sure that either the donor of the third pair is compatible with the recipient of the first pair, or that there exists at least one pair that can complete the cycle.
- An additional set of 4-cycles C_4^3 with exactly three */AB pairs $[X/AB - AB/AB - AB/AB - AB/Y]$, where $X \in \{A, B, AB\}$ and $Y \in \{A, B\}$.

3.4 Bound performance on PrefLib instances

We tested each of the bounds on a set of 30 PrefLib instances without non-directed donors, which is the subset that was used by Lam and Mak-Hau [21] for testing their branch-and-price-and-cut algorithm. The results are available in Table 2. The “Instance” column gives the name of the instance, column n gives the number of recipient/donor pairs in the instance, the four following columns gives the upper bounds and optimal value for $L = 3$, and the last four columns give the same information for $L = 4$. The optimal values were either obtained from [21] or were deduced from a lower bound obtained in [21] combined with one of the upper bounds we introduced.

Table 2: U_1, U_2 , and U_3 values for PrefLib instances with $L = 3$ and $L = 4$

Instance	n	$L = 3$				$L = 4$			
		U_1	U_2	U_3	OPT	U_1	U_2	U_3	OPT
MD-00001-00000191	512	352	352	351	351	352	352	352	352
MD-00001-00000192	512	337	337	337	337	337	337	337	337
MD-00001-00000193	512	300	301	300	300	300	301	300	300
MD-00001-00000194	512	313	313	313	313	313	313	313	313
MD-00001-00000195	512	322	322	322	322	322	322	322	322
MD-00001-00000196	512	313	313	313	313	313	313	313	313
MD-00001-00000197	512	334	337	334	334	334	337	334	334
MD-00001-00000198	512	332	333	332	332	332	333	332	332
MD-00001-00000199	512	313	314	313	313	313	314	313	313
MD-00001-00000200	512	312	313	312	312	312	313	312	312
MD-00001-00000231	1024	659	659	658	658	659	659	659	659
MD-00001-00000232	1024	662	662	662	662	662	662	662	662
MD-00001-00000233	1024	635	636	635	635	635	636	635	635
MD-00001-00000234	1024	641	642	641	641	641	642	641	641
MD-00001-00000235	1024	660	660	660	660	660	660	660	660
MD-00001-00000236	1024	655	655	655	655	655	655	655	655
MD-00001-00000237	1024	597	597	597	597	597	597	597	597
MD-00001-00000238	1024	672	672	671	671	672	672	672	672
MD-00001-00000239	1024	673	674	673	673	673	674	673	673
MD-00001-00000240	1024	639	639	639	639	639	639	639	639
MD-00001-00000271	2048	1284	1284	1284	1284	1284	1284	1284	1284
MD-00001-00000272	2048	1249	1249	1249	1249	1249	1249	1249	1249
MD-00001-00000273	2048	1232	1232	1232	1232	1232	1232	1232	1232
MD-00001-00000274	2048	1242	1242	1242	1242	1242	1242	1242	1242
MD-00001-00000275	2048	1301	1301	1301	1301	1301	1301	1301	1301
MD-00001-00000276	2048	1311	1311	1311	1311	1311	1311	1311	1311
MD-00001-00000277	2048	1316	1316	1316	1316	1316	1316	1316	1316
MD-00001-00000278	2048	1268	1268	1268	1268	1268	1268	1268	1268
MD-00001-00000279	2048	1271	1272	1271	1271	1271	1272	1271	1271
MD-00001-00000280	2048	1295	1295	1295	1295	1295	1295	1295	1295

We observe that bound U_1 displays a very good quality, as it is equal to the optimal solution in 27 instances out of 30 for $L = 3$ and on all instances for $L = 4$. In fact, by simply using U_1 with the solution obtained by the algorithm of Lam and Mak-Hau [21] for $L = 3$, we could solve the 11 benchmark instances with $L = 4$ that they left open in their paper. Upper bound U_2 is also very promising, finding the optimal objective value in 39 instances out of 60. It is not surprising that the values of U_1 and U_2 do not change when the cycle size limit increases as L is not taken into account when the bounds are computed. We also notice that upper bound U_3 displays outstanding performance on the PrefLib instances as it is always equal to the optimal solution value both for $L = 3$ and $L = 4$. It is worth mentioning that each bound was calculated in less than one second of computing time. The experiments were run on an Intel Xeon E5-2680W v3, 2.50GHz with 192GB of memory, running under Scientific Linux 7.5, and using Gurobi 7.5.2 to solve the ILP models.

4 Matheuristic for solving PrefLib instances

Lam and Mak-Hau [21] observed that the cycle formulation obtained poor results on PrefLib instances. This can be explained by the very large number of cycles that have to be generated to run the model due to the cycle size limit ($L = 3$ or 4), the density of the compatibility graph (close to 0.25), and the large number of recipient/donor pairs (from 512 to 2048).

In this section, we introduce a 7-step matheuristic specifically tailored for solving PrefLib instances that takes advantage of the high density in the compatibility graph and of the large number of recipient/donor pairs. When used with upper bound U_3 presented in the previous section, it is able to solve all the tested instances in a few seconds of computing time, which is much faster than the algorithm of Lam and Mak-Hau [21].

Matheuristic is a neologism originating from the contraction of “math” and “heuristic” and is often used as an alternative to mathematical models when the latter become too large to solve difficult combinatorial optimisation problems. Matheuristics usually obtain good quality solutions but do not have a proof of optimality. A common approach in matheuristics is to solve a mathematical model with a reduced set of variables once or several times in a row. In the following, we first describe our matheuristic for $L = 3$ and then we explain how to modify it for $L = 4$.

4.1 Matheuristic overview

As we observed that our best upper bound was tight on the PrefLib instances, the matheuristic aims to find a solution with value U_3 exactly. To do so, it keeps the same assumptions from earlier, namely that every pair participates in the exchange with the exception of ℓ_1 $0/*$ pairs and ℓ'_2 $*/AB$ pairs. It also assumes that no $0/AB$ pairs should be included in the exchange and that every 0 donor should be matched with an 0 recipient. We provide in Algorithm 1 an overview of our approach.

Algorithm 1 7-step matheuristic

- 1: Identify the types of cycles and recipient/donor pairs used in the exchange and process the $AB/*$ and $*/AB$ pairs
 - 2: Process the B/B pairs
 - 3: Process the A/B and B/A pairs
 - 4: Process the A/A pairs
 - 5: Process the $0/0$ pairs
 - 6: Process the $B/0$ and $0/B$ pairs
 - 7: Process the $A/0$ and $0/A$ pairs
-

The matheuristic starts by determining the types of cycles that should be used if a solution of value U_3 (hence optimal) exists (e.g., x_1 cycles of the form $[A/B - B/A]$, x_2 cycles of the form $[A/B - B/0 - 0/A], \dots$). Then, for each combination of recipient/donor pairs, it uses the compatibility graph to enumerate every feasible cycle or partial cycle of the given types and uses an ILP formulation to select those that are necessary to reach the desired solution. At each step, we define:

- An *objective*, which is the goal of the ILP model that is solved at the current step.
- A list of *cycles to complete*, which contains the cycles and incomplete cycles determined at a previous step that need to be completed at the current step if we want to reach a solution of value U_3 because it is the last opportunity to do so.
- A list of *pairs to use*, which contains the pairs that need to be assigned to a cycle at the current step if we want to reach a solution of value U_3 because it is the last opportunity to do so.
- a list of *types of cycles allowed*, which contains the types of cycles that are enumerated in the ILP formulation at the current step;
- A list of *types of incomplete cycles allowed*, which contains the types of incomplete cycles (i.e., with no compatibility requirements between the donor of the second pair and the recipient of the first pair) that are enumerated in the ILP formulation at the current step.

The model is inspired by the cycle formulation (see [29]) and associates a binary variable to every cycle and every incomplete cycle allowed. It maximises the defined “objective” under the constraints

359 that every “cycle to complete” must be completed and every “pair to use” must be assigned to a cycle.
 360 Note that the cycles selected at a given step are assumed to be fixed at each subsequent step while the
 361 partial cycles selected at a given step must be completed (but cannot be broken) in a subsequent step.

362 4.2 Matheuristic steps

363 Step 1: Identifying the types of cycles in the exchange

364 The first step consists of finding how to split the 16 kinds of recipient/donor pairs (4×4 , one for each
 365 possible blood-group combination) into cycle types that our matheuristic will seek in subsequent steps
 366 in order to obtain a solution with value U_3 .

367 Out of these 16 kinds of pairs, we process the AB/* and */AB pairs first as these are critical to finding
 368 a solution with the desired value. Similarly to what was done for U_3 , we enumerate every cycle (complete
 369 or incomplete) containing a */AB pair (i.e., we reuse set $\mathcal{C} = C_2^2 \cup C_3^3 \cup P_2^1 \cup C_3^2$). We also define $P_2^{1,X/Y}$ (X
 370 $\in \{0, A, B\}$, $Y \in \{A, B\}$), a subset of P_2^1 containing every partial cycle $[Y/AB - AB/X]$, meaning that an X/Y
 371 pair might be needed at a later stage to complete the cycle. For practical reasons, cycles $[AB/AB - AB/X]$
 372 are included in the set $P_2^{1,X/A}$, as there are significantly more A donors than A recipients in the PrefLib
 373 instances. We also add the possibility to “transform” any AB/X pair ($X \in \{0, A, B\}$) into a A/X pair or a
 374 B/X pair to allow it to participate in the exchange even if it is incompatible with every */AB pair. The
 375 AB/X pairs are gathered in $\mathcal{V}_{AB/X}$ and the X/AB pairs are gathered in $\mathcal{V}_{X/AB}$, forming all together set \mathcal{V} .

376 Out of the 9 remaining kinds of pairs, we remove the O/O, A/A, and B/B combinations, as we assume
 377 they will always participate in the exchange, either to complete a partial cycle, or to extend a 2-cycle
 378 to a 3-cycle (e.g., an O/O pair used in the middle of an $[A/O - O/A]$ or a $[B/O - O/B]$ cycle), or to form a
 379 cycle with other pairs of the same type. The remaining 6 combinations are spread among the following
 380 5 types of cycles:

- 381 • $[A/B - B/A]$;
- 382 • $[A/O - O/A]$;
- 383 • $[B/O - O/B]$;
- 384 • $[A/B - B/O - O/A]$;
- 385 • $[B/A - A/O - O/B]$.

By using binary decision variables x_c taking value 1 if cycle c is selected and 0 otherwise ($c \in \mathcal{C}$),
 five integer variables x_{ABBA} , x_{A00A} , x_{B00B} , x_{ABB00A} , x_{BAA00B} indicating the number of cycles $[A/B - B/A]$, $[A/O -$
 $O/A]$, $[B/O - O/B]$, $[A/B - B/O - O/A]$, $[B/A - A/O - O/B]$ selected in the exchange, respectively, binary variable
 $t_i^{AB \rightarrow X}$ ($X \in \{A, B\}$, $Y \in \{0, A, B\}$, $i \in \mathcal{V}_{AB/Y}$) taking value 1 if AB/Y pair i is transformed into an X/Y pair,
 the objective function of the ILP model maximising the number of exchanges is defined as follows:

$$386 \max z_1 = \sum_{c \in \mathcal{C}} s_c x_c + 2(x_{ABBA} + x_{A00A} + x_{B00B}) + 3(x_{ABB00A} + x_{BAA00B}) + \sum_{X \in \{0, A, B\}} n_{X/X} + \sum_{\substack{i \in \mathcal{V}_{AB/X} \\ X \in \{A, B\}}} t_i^{AB \rightarrow X}, \quad (4)$$

386 where s_c indicates the size of cycle c , which is 2 if $c \in C_2^2$, 2 if $c \in P_2^{1,A/A} \cup P_2^{1,B/B}$ (even if these cycles
 387 are not necessarily complete, every A/A and B/B pair is counted in the objective function in the second
 388 summation), 3 if $c \in P_2^{1,A/B} \cup P_2^{1,B/A} \cup P_2^{1,O/A} \cup P_2^{1,O/B}$ (these cycles need to be completed by a third pair),
 389 and 3 if $c \in C_3^3 \cup C_3^2$. The last summation adds to the objective function the AB/A pairs transformed
 390 to A/A and the AB/B pairs transformed to B/B (we recall that AB/O pairs cannot be transformed into
 391 O/O pairs as we do not have enough O donors to satisfy the current O recipients in the PrefLib instances).

The six capacity constraints related to each of the six types of pairs of the form A/B, B/A, A/O, O/A,

B/O, O/B are as follows:

$$x_{ABBA} + x_{ABBOOA} + \sum_{c \in P_2^{1,A/B}} x_c \leq n_{A/B} + \sum_{i \in \mathcal{V}_{AB/B}} t_i^{AB \rightarrow A}, \quad (5)$$

$$x_{ABBA} + x_{BAAOOB} + \sum_{c \in P_2^{1,B/A}} x_c \leq n_{B/A} + \sum_{i \in \mathcal{V}_{AB/A}} t_i^{AB \rightarrow B}, \quad (6)$$

$$x_{A00A} + x_{BAAOOB} \leq n_{A/O} + \sum_{i \in \mathcal{V}_{AB/O}} t_i^{AB \rightarrow A}, \quad (7)$$

$$x_{A00A} + x_{ABBOOA} + \sum_{c \in P_2^{1,O/A}} x_c \leq n_{O/A}, \quad (8)$$

$$x_{B00B} + x_{ABBOOA} \leq n_{B/O} + \sum_{i \in \mathcal{V}_{AB/O}} t_i^{AB \rightarrow B}, \quad (9)$$

$$x_{B00B} + x_{BAAOOB} + \sum_{c \in P_2^{1,O/B}} x_c \leq n_{O/B}. \quad (10)$$

For each X/Y combination ($X, Y \in \{O, A, B\}$, $X \neq Y$), a dedicated constraint makes sure that the number of X/Y pairs used in the five types of cycles plus the number of X/Y pairs required to complete the cycles in P_2^1 is less than or equal to the total number of X/Y pairs available plus the number of AB/Y pairs transformed into X/Y pairs. Note that (i) sets $P_1^{A/O}$ and sets $P_1^{B/O}$ do not exist because the matheuristic assumes that no O/AB pairs should be included in the exchange, and (ii) variables $t_i^{AB \rightarrow O}$ do not exist because the matheuristic assumes that every O donor should be matched with an O recipient. The rest of the model is as follows:

$$\sum_{c \in \mathcal{C}: i \in V(c)} x_c + t_i^{AB \rightarrow A} + t_i^{AB \rightarrow B} \leq 1, \quad \forall i \in \mathcal{V}_{AB/O} \cup \mathcal{V}_{AB/A} \cup \mathcal{V}_{AB/B}, \quad (11)$$

$$\sum_{c \in \mathcal{C}: i \in V(c)} x_c \leq 1, \quad \forall i \in \mathcal{V}_{A/AB} \cup \mathcal{V}_{B/AB} \cup \mathcal{V}_{AB/AB}, \quad (12)$$

$$x_c \in \{0, 1\}, \quad \forall c \in \mathcal{C}, \quad (13)$$

$$t_i^{AB \rightarrow A}, t_i^{AB \rightarrow B} \in \{0, 1\}, \quad \forall i \in \mathcal{V}_{AB/O} \cup \mathcal{V}_{AB/A} \cup \mathcal{V}_{AB/B}, \quad (14)$$

$$x_{ABBA}, x_{A00A}, x_{B00B}, x_{ABBOOA}, x_{BAAOOB} \in \mathbb{Z}^+, \quad (15)$$

392 where constraints (11) and (12) ensure that pairs AB/* and */AB can be used at most once. After running
 393 model (4)-(15) on instance “MD-00001-00000191” from the PrefLib repository, we obtain the following
 394 solution:

- 395 • [pair 9 - pair 307], a [B/AB - AB/O] cycle to be completed by an O/B pair,
- 396 • [pair 253 - pair 248], an [A/AB - AB/O] cycle to be completed by an O/A pair,
- 397 • [pair 258 - pair 259], an [AB/AB - AB/O] cycle to be completed by an O/A pair,
- 398 • [pair 306 - pair 91], an [A/AB - AB/A] cycle that may be completed by an A/A pair,
- 399 • [pair 356 - 244], an [A/AB - AB/B] cycle to be completed by a B/A pair,
- 400 • $52 \times [A/B - B/A]$,
- 401 • $51 \times [A/O - O/A]$,
- 402 • $3 \times [B/O - O/B]$,
- 403 • $7 \times [A/B - B/O - O/A]$,
- 404 • $0 \times [B/A - A/O - O/B]$,
- 405 • 34 A/A, 4 B/B, and 66 O/O pairs,

406 • 0 transformation of AB/* pairs,

407 for a total of 351 pairs, which matches bound U_3 ($3 + 3 + 3 + 2 + 3 + 2 \times 106 + 3 \times 7 + 104 = 351$). The
408 partial cycles involving */AB pairs will be carried over to subsequent steps and extended to full cycles.
409 The remainder of the solution indicates the numbers of cycles of the given types that could be computed;
410 attempts to construct the cycles themselves are made in subsequent steps. Note that the solution given
411 by the model can possibly be adjusted to convert two cycles [A/B - B/O - O/A] and [B/A - A/O - O/B] into
412 three cycles [A/B - B/A], [A/O - O/A], and [B/O - O/B] as 2-cycles are easier to handle. We underline that
413 at this point, we are not sure that a solution with value 351 exists: the output of this step is a skeleton
414 solution which, if it can be built up using the subsequent steps, will have value 351.

415 Step 2: Process the B/B pairs

416 In the second step, we deal with B/B pairs. We start by these pairs because B is the least common
417 blood-group in the PrefLib instances apart from AB (already processed in Step 1). At this step:

418 • **Objective:** maximise the number of B/B pairs inserted in a cycle.

419 • **Cycles to complete:** [B/AB-AB/B] (fixed in Step 1).

420 • **Pairs to use:** none.

421 • **Types of cycles allowed:** [B/AB-AB/B], [B/AB-AB/B-B/B], [B/B-B/B], [B/B-B/B-B/B].

422 We identify the structures that were fixed in a previous step by underlining them. We try to find a
423 suitable cycle for as many B/B pairs as possible under the constraint that every [B/AB-AB/B] cycle found
424 in Step 1 should now be completed. This means that either the donor of the second pair is compatible
425 with the recipient of the first pair, or that a B/B pair is needed to complete the cycle. After running Step
426 2 on instance “MD-00001-00000191”, two B/B pairs could be matched into a [B/B-B/B] cycle, meaning
427 that the other two become “pairs to use” in a subsequent step.

428 Step 3: Process the A/B and B/A pairs

429 In the third step, we deal with A/B and B/A pairs:

430 • **Objective:** maximise the number of [A/B-B/A] cycles

431 • **Cycles to complete:** [A/AB-AB/B], [B/AB-AB/A] (fixed in Step 1).

432 • **Pairs to use:** B/B (from Step 2).

433 • **Types of cycles allowed:** [A/AB-AB/B-B/A], [B/AB-AB/A-A/B], [A/B-B/A], [A/B-B/B-B/A].

434 • **Types of incomplete cycles allowed:** [A/B-B/O], [B/A-A/O], [A/B-B/A].

435 We try to find as many [A/B-B/A] cycles as expected under the constraint that some of these cycles should
436 incorporate the “pairs to use” B/B that could not be matched in Step 2, that some pairs A/B and B/A
437 should be used to complete the [B/AB-AB/A] and [A/AB-AB/B] cycles selected in Step 1, and that we have
438 to create the partial cycles [A/B-B/O] (or [B/A-A/O]) that will be completed by O/A pairs at Steps 7 (or
439 by O/B pairs at Step 6). It is also possible to create incomplete cycles [A/B-B/A] that will be completed
440 by an A/A pair at Step 4. After running Step 3 on instance “MD-00001-00000191”, cycle [356-244] was
441 completed, the seven [A/B-B/O] partial cycles were found, and all 52 cycles containing one A/B pair and
442 one B/A pair could be found: 50 [A/B-B/A] 2-cycles and 2 [A/B-B/B-B/A] 3-cycles, the latter containing
443 the two remaining B/B pairs from Step 2.

444 Step 4: Process the A/A pairs

445 In the fourth step, we deal with A/A pairs. At this step:

- 446 • **Objective:** maximise the number of A/A pairs inserted in a cycle.
- 447 • **Cycles to complete:** $[A/AB-AB/A]$ (fixed in Step 1), $[A/B-B/A]$ (fixed in Step 3).
- 448 • **Pairs to use:** none.
- 449 • **Types of cycles allowed:** $[A/AB-AB/A]$, $[A/AB-AB/A-A/A]$ $[B/A-A/A-A/B]$, $[A/A-A/A]$.

450 We try to find a suitable cycle for as many A/A pairs as possible under the constraint that every cycle
451 $[A/AB-AB/A]$ found in Step 1 and cycle $[A/B-B/A]$ found in Step 3 should now be completed. Note that
452 we do not generate the cycles containing three A/A pairs because it makes the model significantly bigger.
453 After running Step 4 on instance “MD-00001-00000191”, 33 out of the 34 A/A pairs could be matched:
454 32 pairs into 16 $[A/A-A/A]$ cycles, and one pair to complete cycle [306-91]. This means that the remaining
455 A/A pair will be dealt with in a subsequent step.

456 Step 5: Process the O/O pairs

457 In the fifth step, we deal with O/O pairs. At this step:

- 458 • **Objective:** maximise the number of O/O pairs inserted in a cycle.
- 459 • **Cycles to complete:** none.
- 460 • **Pairs to use:** none.
- 461 • **Types of cycles allowed:** $[O/O - O/O]$.

462 We try to find a suitable cycle for as many O/O pairs as possible. Note that we do not generate the
463 cycles containing three O/O pairs because it makes the model significantly bigger. After running Step 5
464 on instance “MD-00001-00000191”, all the 66 O/O pairs could be matched into 33 $[O/O-O/O]$ cycles.

465 Step 6: Process the B/O and O/B pairs

466 In the sixth step, we deal with B/O and O/B pairs. We use these pairs at the end of the matheuristic
467 because there are many O/B pairs that will not participate in the exchange due to a lack of O donors. At
468 this step:

- 469 • **Objective:** maximise the number of $[B/O-O/B]$ cycles.
- 470 • **Cycles to complete:** $[B/AB-AB/O]$ (fixed in Step 1), $[B/A-A/O]$ (fixed in Step 3).
- 471 • **Pairs to use:** none.
- 472 • **Types of cycles allowed:** $[B/AB-AB/O-O/B]$, $[B/O-O/B]$, $[B/O-O/O-O/B]$, $[B/A-A/O-O/B]$.

473 We try to find as many $[B/O-O/B]$ cycles as expected under the constraint that some O/B pairs should
474 be used to complete the $[B/AB-AB/O]$ cycles found in Step 1 and that we have to complete the partial
475 cycles $[B/A-A/O]$ from Step 3 with O/B pairs. Note that some $[B/O-O/B]$ cycles could also be used to
476 insert the O/O pairs that could not be matched in Step 5, but there are so few B/O pairs in PrefLib
477 instances that it is not often possible to do so. This also explains why we consider that B/B are “pairs to
478 use” in Step 3 while they could also theoretically be used in this step. After running Step 6 on instance
479 “MD-00001-00000191”, all 3 $[B/O-O/B]$ cycles could be found and cycle [9-307] was completed.

480 **Step 7: Process the A/O and O/A pairs**

481 In the last step, we deal with A/O and O/A pairs. We finish with these pairs because O/A pairs are the
 482 most frequent pairs in PrefLib instances, and many of them will not participate in the exchange due to
 483 the lack of O donors. At this step:

- 484 • **Objective:** maximise the number of [O/A-A/O] cycles.
- 485 • **Cycles to complete:** [A/AB-AB/O] (fixed in Step 1), [O/AB-AB/A] (fixed in Step 1), [A/B-B/O]
 486 (fixed in Step 3).
- 487 • **Pairs to use:** O/O (from Step 5), A/A (from Step 4).
- 488 • **Types of cycles allowed:** [A/AB-AB/O-O/A], [A/O-O/O/A], [A/O-O/O-O/A], [A/O-O/A-A/A], [A/B-B/O-O/A].

489 We try to find as many [O/A-A/O] cycles as expected under the constraint that some of these cycles
 490 should incorporate the “pairs to use” A/A and O/O that could not be matched in Steps 4 and 5, that
 491 some O/A pairs should be used to complete the [A/AB-AB/O] cycles found in Step 1 and that we have to
 492 complete the partial cycles [A/B-B/O] from Step 3 with O/A pairs. Note that it is not necessary to consider
 493 [O/AB-AB/A] cycles as we assumed that O/AB pairs were excluded from the exchange. After running Step
 494 7 on instance “MD-00001-00000191”, cycles [253 – 248] and [258 – 259] were completed, the 7 incomplete
 495 [A/B-B/O] cycles from Step 3 were completed by an O/A pair to form 7 complete [A/B-B/O-O/A] cycles,
 496 all 51 cycles containing one A/O pair and one O/A pair could be found: 50 [A/O-O/A] cycles and one
 497 [A/O-O/A-A/A] cycle, the latter containing the remaining A/A pair from Step 4.

498 **Extending the matheuristic for $L = 4$**

499 We were able to solve the PrefLib instances with $L = 4$ by only updating Step 1 in the same way
 500 we updated U_3 in Section 3, i.e., by updating the set containing the AB/* and */AB pairs as $\mathcal{C} =$
 501 $C_2^2 \cup C_3^3 \cup C_4^4 \cup P_2^1 \cup P_3^2 \cup C_4^3$. It was not necessary to consider any supplementary types of cycles (e.g.,
 502 [B/B-B/A-A/A-A/B] or [O/O-O/O-O/O-O/O]).

503 **4.3 Matheuristic performance on PrefLib instances and discussion**

504 We measured the performance of our matheuristic on the 30 PrefLib instances used by Lam and Mak-
 505 Hau [21] for testing their branch-and-price-and-cut algorithm and the results are displayed in Table 3.
 506 Column “ L ” gives the cycle size limit, column “ n ” gives the number of recipient/donor pairs in the
 507 instance, the three following columns indicate the number of optimal solutions found by the matheuristic
 508 (out of 10), the average lower bound (which was always equal to U_3 in all tested instances), and the
 509 computing time in seconds (using the same computational environment as the one described in Section 3).
 510 The six following columns report the number of optimal solutions found and the computing time required
 511 by the branch-and-price-and-cut and two ILP formulations as reported in the experiments of Lam and
 512 Mak-Hau [21].

Table 3: Matheuristic performance on PrefLib instances

Parameters		Matheuristic			PIEF		PICEF / Cycle		B-P-C	
L	n	OPT	LB	Time	OPT	Time	OPT	Time	OPT	Time
3	512	10	322.7	0.2	10	8	10	82	10	1
3	1024	10	649.1	1.4	4	1304	5	1308	10	0
3	2048	10	1276.9	3.0	0	1800	0	1800	10	5
4	512	10	322.8	0.2	0	1800	0	1800	10	21
4	1024	10	649.3	0.7	0	1800	0	1800	9	800
4	2048	10	1276.9	3.4	0	1800	0	1800	0	1800

513 We observe that the matheuristic can solve every instance in a few seconds. In particular, it is able
 514 to solve the 11 instances left open by Lam and Mak-Hau [21]. Even though these results are very good,
 515 a word of caution is in order: the matheuristic is tailored for large-size PrefLib instances. These are
 516 characterised by a very large graph density (around 25%) and a relatively large number of recipient/donor

517 pairs, which makes it very likely that the cycles predicted in Step 1 can be constructed in subsequent
518 steps. Small-size PrefLib instances could not be solved by the matheuristic but were qualified as “trivial”
519 by Lam and Mak-Hau [21] (i.e., solvable in seconds by an ILP formulation). Real-world instances from
520 the UKLKSS seem to indicate that graph densities are usually smaller (around 10%).

521 The main objective of this section is to show that benchmark instances, which are important for
522 developing new algorithms, can easily favour one kind of algorithm. PrefLib instances have a high graph
523 density, which penalises the methods that enumerate every feasible cycle (such as the cycle formulation
524 and PICEF) and benefits methods using lower and upper bounding techniques (like our matheuristic).
525 In the following, we suggest some improvements for the Saidman generator (that was used for generating
526 the PrefLib instances) in order to make it produce instances that match more closely the real-world
527 instances of the UKLKSS.

528 **5 Improved generation of KE instances**

529 This section introduces a new method for generating KE instances, based on the Saidman generator.
530 This generator, which we describe in Section 5.2, is widely used to generate random KE instances for
531 evaluating both computational techniques and policy changes. We develop a number of improvements
532 to the Saidman generator, and then show that using our refined version creates instances that are
533 substantially closer to the real-world instances from the UK in a number of important measures (such
534 as number of edges or sizes of solutions) when compared to those constructed by the original Saidman
535 generator. Each of our improvements is based on statistical evidence from the UKLKSS, and accompanied
536 by a justification based on real-world scenarios. This is followed by an experimental evaluation of these
537 improvements, and a conclusion discussing the outcomes of the experiments.

538 **5.1 Performance evaluation and data presentation**

539 We evaluate the performance of our improvements by generating random instances and comparing them
540 to real-world data from the UKLKSS. We gathered the blood-group and cPRA distributions from UK-
541 LKSS instances from January 2012 to October 2019 (32 instances in total as UKLKSS runs matchings
542 quarterly), and these are summarised in Appendix A. As these real-world instances do not have a constant
543 size, we cannot report the results of our experiments by comparing the averages of various parameters.
544 Instead, for each real-world instance, we create 20 random instances with the same number of recipients
545 and non-directed donors (the precise number of directed donors is determined by the generator). For
546 each such randomly-generated instance and its associated real-world instance, and for each parameter we
547 measure, we calculate the ratio of the value of parameter in the random instances divided by the value of
548 the parameter in the real-world instance (e.g., if the random instance has 5000 edges, but the real-world
549 instance has 4000 edges, we report the ratio $\frac{5000}{4000} = 1.25$). This results in a set of 640 ratios for each
550 parameter measured. We then plot the distribution of these ratios as box-and-whisker plots. These plots
551 show a coloured box denoting the interquartile range (IQR), a black vertical bar denoting the median,
552 and a white cross denoting the mean. The horizontal lines extend a distance of 1.5 IQR from either side
553 of the coloured box (if no data points extend this far, these lines stop at the last data point), with data
554 points further away being marked as outliers with solid dots. We limit data and plots presented in this
555 section to show only the ratios corresponding to the number of edges in the compatibility graphs and
556 the size of the largest set of identified transplants. We include in Appendix B results on a much larger
557 variety of parameters.

558 **5.2 The Saidman generator**

559 The Saidman generator [30] is widely used to generate instances of KEP problems [12, 19]. We now
560 describe how the Saidman generator functions, and then compare the output from the Saidman generator
561 to real world instances.

562 **5.2.1 Generation process**

563 The Saidman generator takes as input the number of recipients, the number of non-directed donors,
564 as well as the distributions of the donor and recipient blood-groups (these may be identical, if distinct

distributions are not known), the distribution of number of donors per recipient¹ and the distribution of cPRA values of the recipients. These distributions are commonly gathered from a long-running KEP; we will be using values from the UKLKSS. The Saidman generator first produces donor-recipient pairs by independently drawing a blood-group and cPRA for a new recipient, as well as drawing the number of donors paired with this recipient, and a blood-group for each of these donors.

For any donor and recipient, their compatibility is determined as follows:

1. If the donor is blood-group incompatible with a given recipient, then they are not compatible.
2. Otherwise, draw uniformly at random a number r from $[0, 1]$. The donor and recipient are compatible if and only if $r > \frac{cPRA}{100}$.

If a donor is determined to be compatible with their paired recipient, the Saidman generator will discard both the recipient and all paired donors to avoid the generation of compatible pairs. Whilst never specifically addressed in the literature, it is commonly accepted that this is done so that the pool of donor-patient pairs more accurately reflects the real-world data. For instance, the proportion of type AB recipients in kidney exchange pools is often lower than the proportion of people with type AB in a general population, as it is easier for type AB recipients to find a willing and compatible donor as they are blood-group compatible with all potential donors. Discarding compatible pairs mimics this effect, and similar effects for recipients with a low cPRA.

Once sufficient recipients have been generated, the Saidman generator then draws a blood-group for each non-directed donor required.

Once this is complete, the compatibility of any donor with any recipient (other than their paired recipient, if applicable) is determined using the above algorithm, and a corresponding arc is added to the compatibility graph if the donor and recipient are compatible.

There are two important factors to note when discussing the Saidman generator. Firstly, the blood-groups of donors and recipients and the cPRA values are all assumed to be independent. This is but one of the aspects we will address later in this section. Secondly, the discarding of compatible pairs means that the distributions of the generated data will not match the input distributions (i.e., low cPRA recipients are more likely to be discarded, so low cPRA recipients will be under-represented in the generated data). To avoid this, the inputs to the Saidman generator can be tuned. This can be achieved by running the generator to produce an instance which is then analysed for some property or set of properties (e.g., the distribution of cPRA levels amongst recipients). If this property is deemed not sufficiently close to some desired target (e.g., the proportion of recipients with a low cPRA is deemed too low), then the inputs can be adjusted (e.g., the probability of a recipient drawing a low cPRA can be increased), and the process is repeated. Alternative tuning options include sweeping across a broad range of parameters to find the input distributions that give output distributions deemed best [31]. In this paper, we tune the distributions of donor blood-groups, recipient blood-groups, recipient cPRA levels, and number of donors paired with a recipient.

5.2.2 Performance of the Saidman generator

Recall from Section 5.1 that we generate 640 random instances, and for each random instance and each parameter we calculate the ratio comparing the parameter in the random instance to the parameter in the real-world instance with the same size. Figure 3 gives boxplots of these ratios for two parameters, showing how the Saidman generator compares to the real-world data. Better generators therefore have means and medians closer to one, and with less variance, although some variance is to be expected. We see that the Saidman generator produced instances with substantially more edges than present within the UKLKSS data, which corresponds to more transplants in a largest set of transplants. A comparison of a larger set of parameters is given in Appendix B.

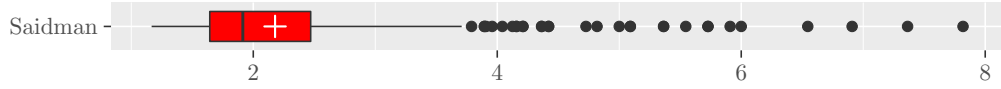
5.3 New generator configurations

In the rest of this section we introduce changes based on three different assumptions made by the Saidman generator. These are: the independence of donor and recipient blood-groups and the recipient cPRA, the

¹The UKLKSS, and many other KEPs, allows a recipient to join a KEP with multiple donors, so as to increase their probability of finding a match.



(a) Distribution of the ratio of number of edges in randomly generated instances



(b) Distribution of the ratio of largest set of transplants in randomly generated instances.

Figure 3: Boxplots outlining the performance of the Saidman generator

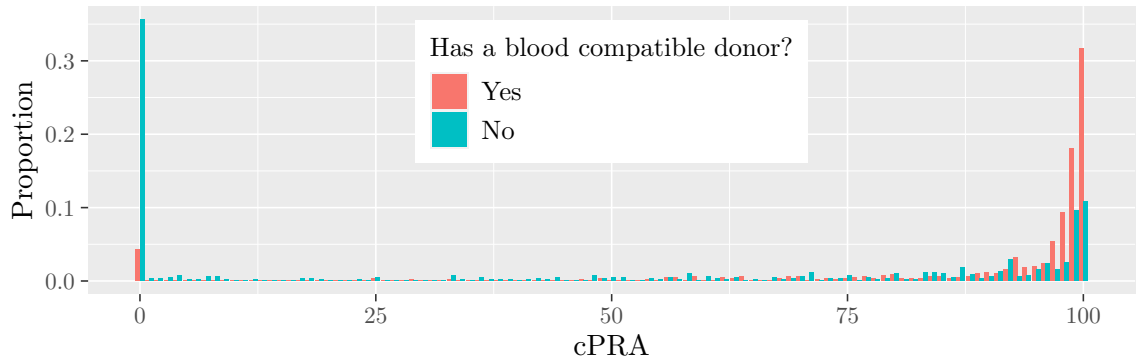


Figure 4: Distributions of cPRA dependent on whether a recipient has a blood-group compatible donor

613 direct linear relationship between cPRA and donor compatibility, and the equivalence of all recipients
 614 with a given cPRA value.

615 5.3.1 Donor and recipient blood-groups and cPRA distributions

616 As noted earlier, the Saidman generator assumes that the blood-groups of the donors and recipients, and
 617 the cPRA levels of the recipients, are independent. From a clinical point of view, however, it would not be
 618 surprising that recipients paired with blood-group compatible donors would be more likely to have tissue-
 619 type incompatibility, as donors and recipients who are both blood-group and tissue-type compatible are
 620 likely to be medically compatible and thus have proceeded with a transplant outside of a KEP. We ran
 621 a t -test of the corresponding Wald statistic [10] to compare our hypothesis that there is a correlation
 622 between a recipient having a blood-group compatible donor and the recipient’s cPRA level against a
 623 null hypothesis. The resulting p -value of approximately 1.79×10^{-7} is a strong indicator that we can
 624 reject the null hypothesis, suggesting that different cPRA distributions should be used when generating
 625 recipients depending on whether a recipient has been generated with a blood-group compatible donor or
 626 not. We show in Figure 4 the distributions of cPRA levels of recipients from the UKLKSS broken down
 627 according to whether or not the recipient is paired with a blood-group compatible donor.

628 An obvious requirement for modelling this phenomenon is the ability to accurately model the correct
 629 proportion of blood-group compatible pairs. To achieve this, we calculate the distribution of blood-
 630 groups of the recipients. We then calculate five distributions of donor blood-groups, one for each of the
 631 four possible recipient blood-groups, and one for non-directed donors. This data is shown in Figure 5,
 632 and we see that there are substantial differences between these distributions.

633 We implement a generator that includes these adaptations, and use the term SplitPRA to refer to
 634 this adaptation. Two box plots comparing the performance of the adaptation SplitPRA to the Saidman
 635 generator are shown in Figure 6. We see from these that SplitPRA creates random instances that are

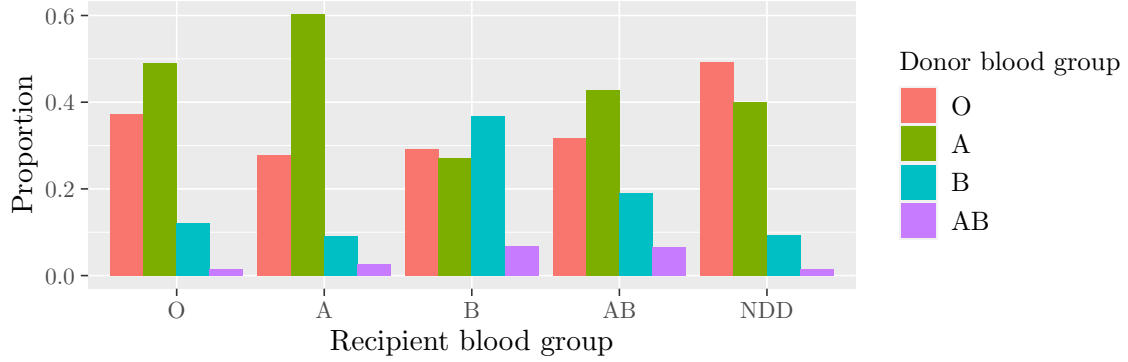
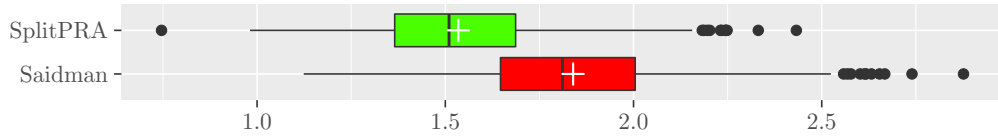
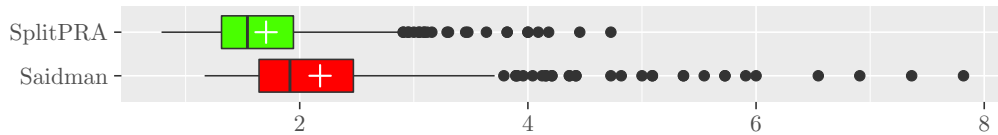


Figure 5: Distributions of donor blood-group by recipient blood-group



(a) Distribution of number of edges as proportion of edges in real-world instances



(b) Size of largest set of transplants

Figure 6: Comparison of Saidman and SplitPRA generators

636 closer to the real-world instances than those produced by the Saidman generator both in terms of number
 637 of edges and size of largest set of transplants.

638 5.3.2 Link between cPRA and transplant compatibility

639 For any donor and recipient who are blood-group compatible, the Saidman generator uses cPRA as
 640 a proxy for transplant compatibility. In real-world applications, transplant compatibility does require
 641 tissue-type compatibility (and cPRA is a good measure of this), but there are also external factors such
 642 as the size of the kidney, or the age or overall health of the donor. As such factors are much harder
 643 to randomly sample, the Saidman generator draws transplant compatibility uniformly at random with
 644 probability $(1 - \text{cPRA}/100)$. However, cPRA by definition only considers tissue-type compatibility, and
 645 ignores these other possible causes of incompatibility that may arise. For each recipient in the UKLKSS
 646 data, we calculate the proportion of blood-group compatible donors appearing in a matching run simul-
 647 taneously with the recipient that are also identified as potential donors for the recipient. We plot
 648 this data in Figure 7. From this, it is clear to see that while there is a strong negative relationship
 649 between cPRA and compatibility (confirmed with a Spearman rank correlation coefficient of approx-
 650 imately -0.519 , which corresponds to a p -value of $< 2.2 \times 10^{-16}$), it is not necessarily as simple as
 651 $(1 - \text{cPRA}/100)$. Indeed, a linear least-squares model weighted by the distribution of cPRA amongst
 652 the recipients gives the equation $P(\text{Compat.}) = 0.58 - 0.55 \times \text{cPRA}/100$. This linear model is shown
 653 as a solid blue line in Figure 7, with the shaded region showing the 95% confidence interval. The tri-
 654 angles denote each data point, with one data point per cPRA value. Note that the number of samples
 655 represented by each data point is not visually represented in Figure 7 to make the plot easier to read.

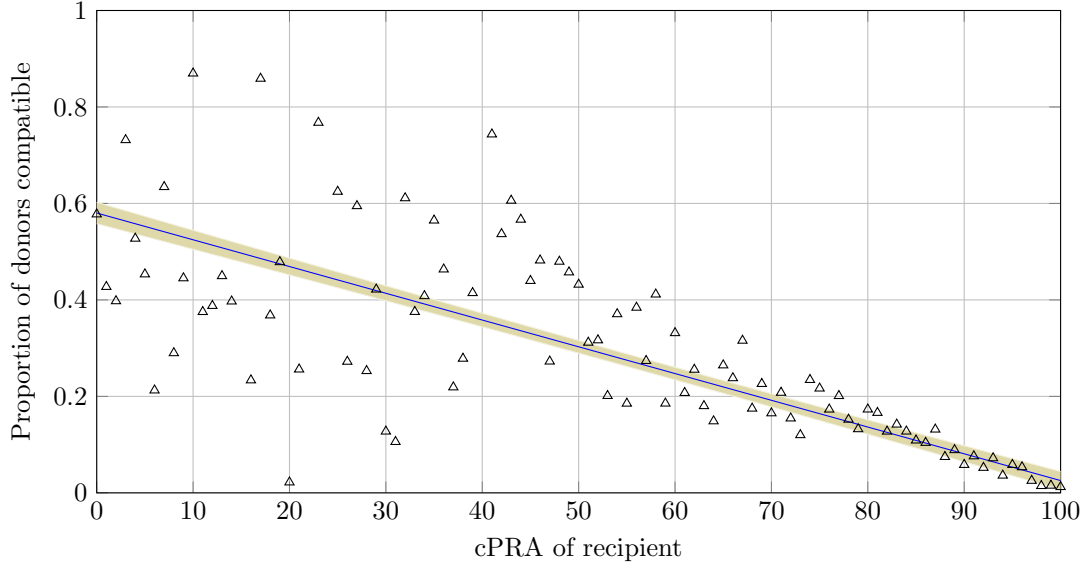


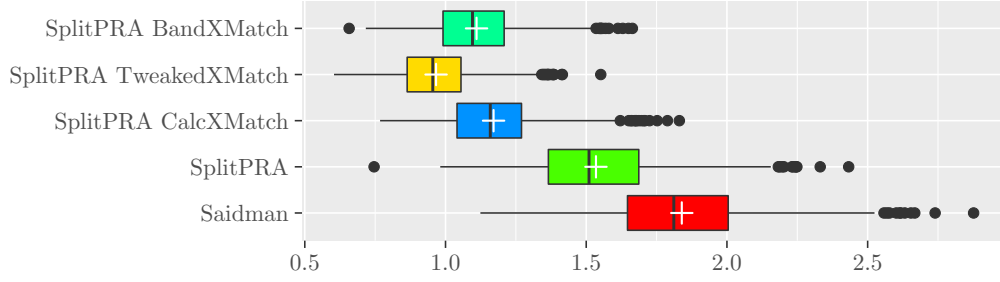
Figure 7: Proportion of UKLKSS donors that are compatible with a blood-group compatible recipient

As such, the reader should be aware that the level of correlation between cPRA and the variance of compatibility as seen in Figure 7 may be misleading. By looking at the data we see that while there is a greater variance at lower values of cPRA (we discuss this in detail for recipients with a cPRA of exactly 0 in Section 5.3.3), much of the variance visually depicted in Figure 7 is due to the relative difference in populations represented at each cPRA value (c.f. Figure 4 which shows the relative distribution of cPRA values among recipients).

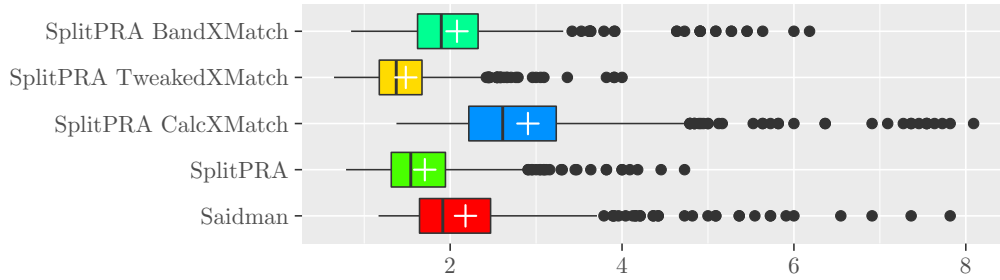
We see that this linear model does approximate the relationship between cPRA and compatibility, but many data points are outside the 95% confidence interval. We also highlight that recipients with a cPRA of 0 (i.e., those recipients who theoretically should have no tissue-type compatibility problems) are only compatible with approximately 58% of the blood-compatible donors in their matching runs. We investigate this particular aspect further in Section 5.3.3. Other studies model the link between cPRA and tissue-type compatibility through the cumulative distribution function (CDF) of a standard normal distribution [17]. However, these studies only consider tissue-type compatibility, whereas we are aiming to model actual compatibility, giving one potential explanation for this difference. Based on the data we observe in Figure 7, neither a linear relationship nor CDF nor any straight-forward model can accurately represent the link between cPRA and transplant compatibility, so we opt for the linear model which is able to more closely match the low but non-zero probability of compatibility that is observed with recipients with a cPRA of 100.

We test an adaptation to the generator that uses $P(\text{Compat.}) = 0.58 - 0.55 \times \text{cPRA}/100$ (i.e., the linear least-squares model) to determine compatibility between blood-compatible donors and recipients; we call this CalcXMatch. Full experimental results are shown in Appendix B, but Figure 8 shows that CalcXMatch does reduce the number of edges (bringing it closer to the real-world instances) but at the cost of significantly increasing the number of transplants identified. A closer examination of the compatibility equation shows that CalcXMatch will give recipients with a cPRA of 100 a 3% chance of compatibility, whereas the Saidman generator gives such recipients a 0% chance of compatibility. Thus, CalcXMatch has fewer incoming edges from the recipients with a low cPRA, and more incoming edges to recipients with cPRA values above 98, compared to the Saidman generator, resulting in more identified transplants.

We test a second adaptation that uses the formula $P(\text{Compat.}) = 0.55 - 0.55 \times \text{cPRA}/100$ to determine compatibility (forcing recipients with a cPRA of 100 to have a 0% chance of compatibility). We call this adaptation TweakXMatch, and its performance is included in Figure 8. This, as expected, reduces the number of edges, but brings the mean number of edges very close to the mean number of edges in the real-world data. Whilst this looks impressive, we do highlight that this particular generator, like the Saidman generator and just using SplitPRA, gives a recipient with a cPRA of 100 zero chance of being



(a) Distribution of number of edges as proportion of edges in real-world instances



(b) Size of largest set of transplants

Figure 8: Comparison of four methods of calculating compatibility

690 compatible, and so no recipients with a cPRA of 100 are ever identified for transplantation.

691 We also create a third adaptation that does not use one equation to determine compatibility for
 692 all recipients. Instead, we split the range of potential cPRA values into the bands $[0, 50)$, $[50, 95)$,
 693 $[95, 96)$, $[96, 97)$, $[97, 98)$, $[98, 99)$, $[99, 100)$ and 100. Then a linear regression is performed on the real-
 694 world recipients from the UKLKSS who fit into each band of cPRA values, giving one equation (or
 695 value, if the band contains just one cPRA value) per cPRA band. These equations are then used to
 696 determine compatibility for generated recipients, based on their cPRA values. We call this configuration
 697 BandXMatch, and its performance is also included in Figure 8. We see that, as expected, it has a similar
 698 number of edges to CalcXMatch, but on average it has a smaller-sized largest set of transplants.

699 5.3.3 The compatibility of cPRA 0 recipients

700 One oddity that arises from Figure 7 is that recipients with a cPRA of 0 are only compatible with
 701 approximately 58% of their blood-group compatible donors. This is somewhat less than may have been
 702 anticipated, so we investigated it further. Figure 9 shows a histogram of the compatibility of real-world
 703 recipients with a cPRA of 0, where compatibility is calculated as the proportion of potential transplants
 704 in the instances divided by the number of blood-group compatible donors in said instances. We see that
 705 approximately 18% of these cPRA 0 recipients are compatible with all of their blood-group compatible
 706 donors, and that approximately 40% of these recipients are compatible with at least 95% of their blood-
 707 group compatible donors. However, almost 26% of recipients with a cPRA of 0 are compatible with less
 708 than 25% of their blood-compatible donors.

709 Some hypotheses have been presented for this phenomenon:

- 710 • Paediatric recipients may have stricter compatibility requirements, beyond the simple blood and
 711 tissue-type compatibility, or,
- 712 • if a recipient is known to have a low (or zero) cPRA, then this recipient (or their clinician) may be
 713 more stringent with regards to other parameters such as age or health of the donor.

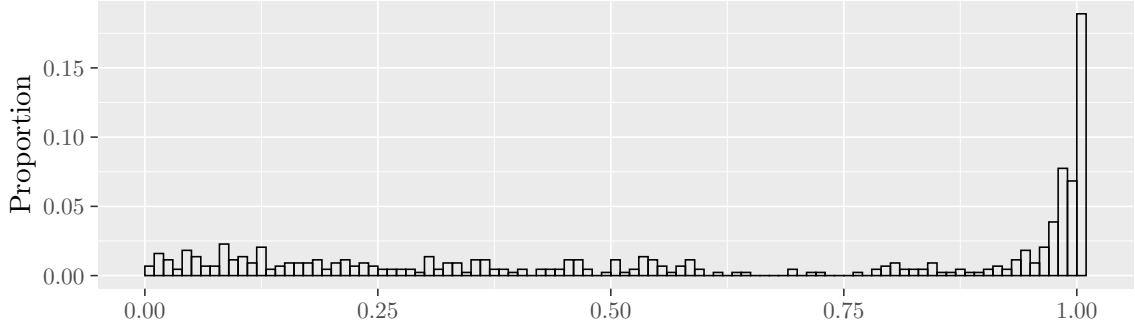


Figure 9: Histogram of compatibility for cPRA 0 recipients

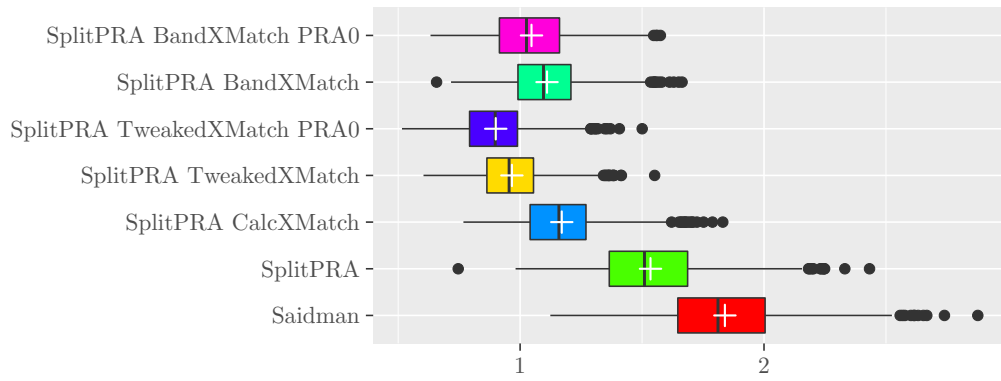
714 We account for this phenomenon in our generator as follows. For each recipient with a cPRA of 0,
 715 we randomly sample from a smoothed variant of the distribution shown in Figure 9 the compatibility
 716 proportion of this recipient. This compatibility proportion is then used directly as the probability that the
 717 recipient is compatible with a blood-group compatible donor. In this way, we generate instances wherein
 718 approximately 40% of recipients with a cPRA of 0 are compatible with over 95% of their blood-group
 719 compatible donors, and so on.

720 Figure 10 shows the performance of this adaptation, which we denote by PRA0 in the plots. We see
 721 that when combined with either TweakXMatch or BandXMatch, this adaptation slightly reduces both
 722 the number of edges and size of the largest set of transplants.

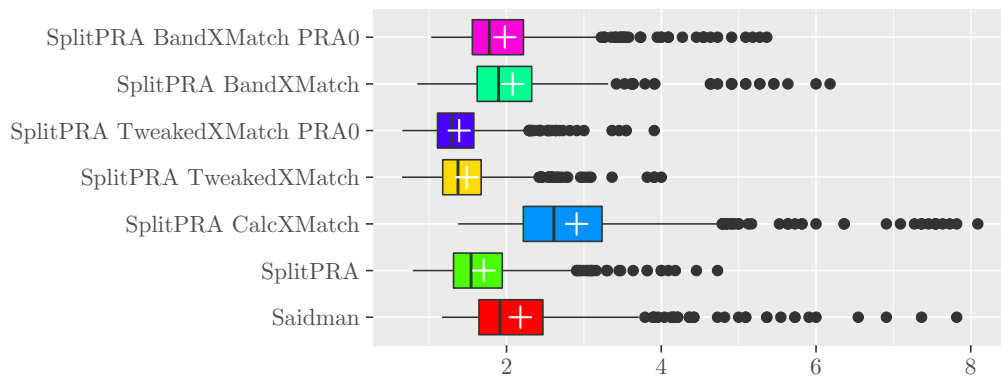
723 5.4 Discussion

724 We have demonstrated a number of improvements to the process of generating random KE instances.
 725 We have shown that the recipients who have a blood-group compatible donor have a markedly different
 726 distribution of cPRA values to those who do not have a blood-group compatible donor, and that utilising
 727 this when generating instances will result in random instances that more closely resemble real-world
 728 instances. This approach can be utilised by simply calculating and using two distinct cPRA distributions
 729 for the two populations. We have also shown that the correlation between cPRA and transplant com-
 730 patibility, whilst present, is not necessarily as simple as $P(\text{compatibility}) = 1 - \text{cPRA}/100$, and taking
 731 a more nuanced approach results in random instances that more closely resemble real-world instances.
 732 Lastly, we show that, within the UKLKSS, recipients with a cPRA of 0 have an unusual distribution of
 733 transplant compatibility. Figure 10 shows that two particular combinations of improvements, SplitPRA
 734 TweakXMatch PRA0 and SplitPRA BandXMatch PRA0, give the best performance. It is important to
 735 note that, while both Figure 10 and further plots in Appendix B show that SplitPRA TweakXMatch
 736 PRA0 generally produces instances with properties closer to instances from the UKLKSS, SplitPRA
 737 TweakXMatch PRA0 gives recipients with a cPRA of 100 zero chance of finding a compatible donor,
 738 while SplitPRA BandXMatch PRA0 gives each such recipient approximately 1% chance of being com-
 739 patible with each blood-compatible donor in the pool. With that in mind, to simulate the UKLKSS, we
 740 recommend the use of SplitPRA BandXMatch PRA0.

741 We ran the first step of the matheuristic from Section 4 on instances generated with our new methods,
 742 and the bound obtained was generally found to be far above the optimal solution (e.g., the maximum
 743 number of transplants, as determined by the cycle formulation, was 364.1 on average for 20 instances
 744 with 1024 recipient/donor pairs while the matheuristic was looking for a solution with value 668.2 on
 745 average). This indicates that, in such instances, the maximum number of transplants does not solely
 746 depend on the blood groups anymore, which explains why the value was overestimated in Step 1 of our
 747 approach. Note that one could update the matheuristic to find a feasible solution even if it does not
 748 match the bound found in Step 1 by modelling the “pairs to use” and the “cycles to complete” as parts of
 749 the objective function instead of within constraints. Even though such an adaptation could potentially
 750 provide good-quality solutions, the lack of a guarantee of optimality would be a major drawback, as exact
 751 approaches are strongly favoured for optimisation problems where the objective function may impact on



(a) Distribution of number of edges as proportion of edges in real-world instances



(b) Size of largest set of transplants

Figure 10: Comparison of all six new methods of calculating compatibility

752 human lives.

753 Many of the conclusions we have drawn are based on a study of UK data, but we expect that at
754 least some of our adaptations (in particular, highlighting the correlation between blood compatibility
755 and cPRA distributions, and the relationship between cPRA and transplant compatibility) will be useful
756 when generating random instances for other KEPs.

757 6 Conclusion

758 We have presented new upper bounds and new matheuristic for identifying large sets of transplants in KE
759 instances. We show that, on a standard set of randomly-generated instances, combining our upper bound
760 and our matheuristic achieves optimal solutions much faster than any algorithm from the literature. This
761 particular set of instances, despite its common use in the literature, differs from real-world instances in a
762 number of vital characteristics (particularly edge density), and our upper bound and matheuristic are not
763 guaranteed to converge, and indeed do not converge, on all real-world instances. We then demonstrated
764 a number of improvements to the standard method of generating random KE instances which are shown
765 to produce instances that are much closer to real-world instances in many characteristics. We have made
766 our generator, and relevant distributions and parameters from the UKLKSS available to allow people to
767 test both new KEP algorithms and new KEP policies on data that closely matches real-world instances
768 from the UKLKSS.

769 We hope to continue work with this generator by collaborating with other KEPs to determine which
770 adaptations are applicable globally and obtain new adaptations for improved generation of KE instances.

771 Acknowledgements

772 The authors would like to thank NHS Blood and Transplant for sharing their data and experience with
773 us. This research was supported by the Engineering and Physical Science Research Council through
774 grant numbers EP/P028306/1 (Manlove and Pettersson), EP/P029825/1 (Delorme, Garcia, Gondzio,
775 and Kalcsics), and EP/R513222/1 (Trimble).

776 References

- 777 [1] D.J. Abraham, A. Blum, and T. Sandholm. Clearing algorithms for barter exchange markets:
778 enabling nationwide kidney exchanges. In *Proceedings of EC '07: the 8th ACM Conference on*
779 *Electronic Commerce*, pages 295–304. ACM, 2007.
- 780 [2] F. Alvelos, X. Klimentova, and A. Viana. Maximizing the expected number of transplants in kidney
781 exchange programs with branch-and-price. *Annals of Operations Research*, 272(1-2):429–444, 2019.
- 782 [3] R. Anderson, I. Ashlagi, D. Gamarnik, and A.E. Roth. Finding long chains in kidney exchange
783 using the traveling salesman problem. *Proceedings of the National Academy of Sciences*, 112:663–
784 668, 2015.
- 785 [4] I. Ashlagi and A. Roth. Individual rationality and participation in large scale, multi-hospital kidney
786 exchange. In *Proceedings of EC '11: the 12th ACM Conference on Electronic Commerce*, pages
787 321–322. ACM, 2011.
- 788 [5] I. Ashlagi and A. Roth. New challenges in multihospital kidney exchange. *American Economic*
789 *Review*, 102(3):354–59, 2012.
- 790 [6] D. A. Axelrod, M. A. Schnitzler, H. Xiao, W. Irish, E. Tuttle-Newhall, S.-H. Chang, B. L. Kasiske,
791 T. Alhamad, and K. L. Lentine. An economic assessment of contemporary kidney transplant
792 practice. *American Journal of Transplantation*, 18:1168–1176, 2018.
- 793 [7] P. Biró, M. Gyetvai, X. Klimentova, J. Pedroso, W. Pettersson, and A. Viana. Compensation scheme
794 with Shapley value for multi-country kidney exchange programmes. In M. Steglich, C. Mueller,
795 G. Neumann, and M. Walther, editors, *Proceedings of the 34th International ECMS Conference*

- 796 *on Modelling and Simulation, ECMS 2020, Wildau, Germany, June 9-12, 2020*, pages 129–136.
797 European Council for Modeling and Simulation, 2020.
- 798 [8] P. Biró, B. Haase-Kromwijk, T. Andersson, E. I. Ásgeirsson, T. Baltsová, I. Boletis, C. Bolotinha,
799 G. Bond, G. Böhmig, L. Burnapp, K. Cechlárová, P. Di Ciaccio, J. Froněk, K. Hadaya, A. Hemke,
800 C. Jacquelinet, R. Johnson, R. Kieszek, D. R. Kuypers, R. Leishman, M.-A. Macher, D. Manlove,
801 G. Menoudakou, M. Salonen, B. Smeulders, V. Sparacino, F. C. R. Spieksma, M. O. Valentín,
802 N. Wilson, and J. van der Klundert. Building Kidney Exchange Programmes in Europe — An
803 Overview of Exchange Practice and Activities. *Transplantation*, 103:1514–1522, 2019.
- 804 [9] P. Biró, J. van de Klundert, D. Manlove, W. Pettersson, T. Andersson, L. Burnapp, P. Chromy,
805 P. Delgado, P. Dworzak, B. Haase, A. Hemke, R. Johnson, X. Klimentova, D. Kuypers, A. Costa,
806 B. Smeulders, F. Spieksma, M. Valentin, and A. Viana. Modelling and optimisation in European
807 Kidney Exchange Programmes. *European Journal of Operational Research*, 291(2):447–456, 2019.
- 808 [10] A. Buse. The likelihood ratio, Wald, and Lagrange multiplier tests: An expository note. *The
809 American Statistician*, 36(3a):153–157, 1982.
- 810 [11] M. Carvalho, X. Klimentova, K. Glorie, A. Viana, and M. Constantino. Robust models for the
811 kidney exchange problem. *INFORMS Journal on Computing*, 2020.
- 812 [12] M. Constantino, X. Klimentova, A. Viana, and A. Rais. New insights on integer-programming
813 models for the kidney exchange problem. *European Journal of Operational Research*, 231:57–68,
814 2013.
- 815 [13] J. Dickerson, D. Manlove, B. Plaut, T. Sandholm, and J. Trimble. Position-indexed formulations
816 for kidney exchange. In *Proceedings of the 2016 ACM Conference on Economics and Computation*,
817 EC ’16, pages 25–42, New York, NY, USA, 2016. ACM.
- 818 [14] J. Dickerson, A.D. Procaccia, and T. Sandholm. Optimizing kidney exchange with transplant
819 chains: Theory and reality. In *Proceedings of AAMAS ’12: the 11th International Conference on
820 Autonomous Agents and Multiagent Systems*, volume 2, pages 711–718. International Foundation
821 for Autonomous Agents and Multiagent Systems, 2012.
- 822 [15] J. Edmonds. Paths, trees, and flowers. *Canadian Journal of Mathematics*, 17:449–467, 1965.
- 823 [16] K. Glorie. Estimating the probability of positive crossmatch after negative virtual crossmatch.
824 Technical Report EI 2012-25, December 2012.
- 825 [17] K. Glorie. *Clearing Barter Exchange Markets: Kidney Exchange and Beyond*. PhD thesis, November
826 2014.
- 827 [18] A. Hart, J. M. Smith, M. A. Skeans, S. K. Gustafson, D. E. Stewart, W. S. Cherikh, J. L. Wainright,
828 A. Kucheryavaya, M. Woodbury, J. J. Snyder, B. L. Kasiske, and A. K. Israni. OPTN/SRTR 2015
829 annual data report: Kidney. *American Journal of Transplantation*, 17:21–116, 2017.
- 830 [19] X. Klimentova, J. Pedroso, and A. Viana. Maximising expectation of the number of transplants in
831 kidney exchange programmes. *Computers & Operations Research*, 73:1–11, 2016.
- 832 [20] H. W. Kuhn. The Hungarian method for the assignment problem. *Naval Research Logistics Quar-*
833 *terly*, 2(1-2):83–97, 1955.
- 834 [21] E. Lam and V. Mak-Hau. Branch-and-cut-and-price for the cardinality-constrained multi-cycle
835 problem in kidney exchange. *Computers & Operations Research*, 115(104852), 2020.
- 836 [22] Z. Li, N. Gupta, S. Das, and J. Dickerson. Equilibrium behavior in competing dynamic match-
837 ing markets. In *Proceedings of the Twenty-Seventh International Joint Conference on Artificial
838 Intelligence, IJCAI-18*, pages 389–395. International Joint Conferences on Artificial Intelligence
839 Organization, 7 2018.
- 840 [23] D. Manlove and G. O’Malley. Paired and altruistic kidney donation in the UK: Algorithms and
841 experimentation. *ACM J. Exp. Algorithmics*, 19, 1 2015.

- 842 [24] N. Mattei and T. Walsch. Preflib.org: A library for preferences. [https://www.preflib.org/data/
843 matching/kidney/](https://www.preflib.org/data/matching/kidney/) (accessed 23 September 2020), 2020.
- 844 [25] D. McElfresh, H. Bidkhor, and J. Dickerson. Scalable robust kidney exchange. *Proceedings of the
845 AAAI Conference on Artificial Intelligence*, 33(01):1077–1084, 7 2019.
- 846 [26] R. Mincu, P. Biró, M. Gyetvai, A. Popa, and U. Verma. IP solutions for international kidney
847 exchange programmes. *Central European Journal of Operations Research*, pages 1–21, 2020.
- 848 [27] W. Mulley and J. Kanellis. Understanding crossmatch testing in organ transplantation: A case-based
849 guide for the general nephrologist. *Nephrology*, 16(2):125–133, 2011.
- 850 [28] A.E. Roth, T. Sönmez, and M.U. Ünver. Kidney exchange. *Quarterly Journal of Economics*,
851 119(2):457–488, 2004.
- 852 [29] A.E. Roth, T. Sönmez, and M.U. Ünver. Efficient kidney exchange: Coincidence of wants in a
853 market with compatibility-based preferences. *American Economic Review*, 97(3):828–851, 2007.
- 854 [30] S.L. Saidman, A.E. Roth, T. Sönmez, M.U. Ünver, and S.L. Delmonico. Increasing the opportunity
855 of live kidney donation by matching for two and three way exchanges. *Transplantation*, 81(5):773–
856 782, 2006.
- 857 [31] N. Santos, P. Tubertini, A. Viana, and J. P. Pedroso. Kidney exchange simulation and optimization.
858 *Journal of the Operational Research Society*, 68(12):1521–1532, 2017.
- 859 [32] R. A. Wolfe, E. C. Roys, and R. M. Merion. Trends in organ donation and transplantation in the
860 United States, 1999–2008. *American Journal of Transplantation*, 10:961–972, 2010.

A Parameters for generating instances similar to real-world instances from the UKLKSS

In this section we list a number distributions relevant to the generation of random instances of KEP problems. These distributions are all taken from the UKLKSS between 2012 and 2018 inclusive. For more details on how these may be used, see Section 5.

Table 4 shows the distribution of number of donors paired with a recipient in the UKLKSS. Recall that in the UKLKSS a donor can be paired with at most one recipient, while a recipient may be paired with multiple donors. In any exchange, only one donor of a recipient is selected (unless the donor is not-directed, in which case they have no paired donor).

Table 4: Distribution of number of donors paired with a recipient in UKLKSS

Number of donors	Proportion
1	0.9112
2	0.0769
3	0.0105
4	0.0015

Table 5 shows the distribution of blood groups amongst recipients within the UKLKSS. Tables 6, 7, 8, and 9 then show the distribution of donor blood groups within the UKLKSS. These distributions are dependent on the blood group of a paired recipient. Table 10 shows the distribution of blood groups amongst non-directed (altruistic) donors within the UKLKSS.

Table 5: Blood group distribution of recipients in the UKLKSS

Blood group	Proportion
O	0.6293
A	0.2325
B	0.1119
AB	0.0263

Table 6: Blood group distribution of donors paired with a recipient with blood group O

Blood group	Proportion
O	0.3721
A	0.4899
B	0.1219
AB	0.1610

Table 11 shows the distribution of cPRA amongst recipients who are paired with at least one blood-group compatible donor. Table 12 shows the distribution of cPRA amongst recipients who are not paired with any blood-group compatible donor. Table 13 shows the relationship between cPRA and likelihood of transplant compatibility with a blood-group compatible donor within the UKLKSS. Where an equation is given, these were determined by linear regression. Table 14 shows the distribution of likelihood of a transplant being incompatible for recipients within the UKLKSS with a cPRA of 0.

B Additional comparisons of various generators

In this section we give extensive results on our tests of various generator configurations. Recall that for each real-world instance, we generated 20 random instances for each of our test generators with the same number of recipients as the corresponding real-world instance. We then calculate, for each

Table 7: Blood group distribution of donors paired with a recipient with blood group A

Blood group	Proportion
O	0.2783
A	0.6039
B	0.0907
AB	0.0270

Table 8: Blood group distribution of donors paired with a recipient with blood group B

Blood group	Proportion
O	0.2910
A	0.2719
B	0.3689
AB	0.0683

parameter, the proportion of the value of the parameter in each random instance divided by the value of the parameter for the real-world instance. These are then plotted as box-and-whisker plots, with a coloured box denoting the interquartile range (IQR), a black vertical bar denoting the median, and a white cross denoting the mean. The horizontal lines extend up to a distance of 1.5 IQR from either side of the coloured box (if no data points extend this far, these lines stop at the last data point), with data points further away being marked as outliers with solid dots.

See Section 5.1 for a more detailed explanation.

Table 9: Blood group distribution of donors paired with a recipient with blood group AB

Blood group	Proportion
O	0.3166
A	0.4271
B	0.1910
AB	0.0653

Table 10: Blood group distribution of non-directed (altruistic) donors in the UKLKSS

Blood group	Proportion
O	0.3333
A	0.2698
B	0.0635
AB	0.0095

Table 11: Distribution of cPRA amongst recipients who have a blood-group compatible paired donor in the UKLKSS

cPRA range	Proportion
0	0.0435
[1, 10)	0.0064
[10, 20)	0.0027
[20, 30)	0.0060
[30, 40)	0.0084
[40, 50)	0.0107
[50, 60)	0.0217
[60, 70)	0.0291
[70, 80)	0.0391
[80, 85)	0.0257
[85, 90)	0.0308
90	0.0114
91	0.0107
92	0.0157
93	0.0318
94	0.0191
95	0.0197
96	0.0241
97	0.0535
98	0.0929
99	0.1802
100	0.3170

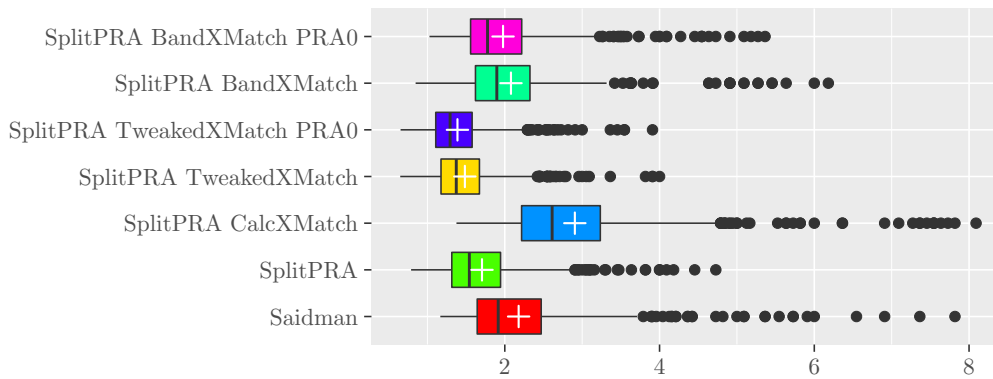


Figure 11: Size of largest set of transplants as a proportion of the size of largest set in real-world instances

Table 12: Distribution of cPRA amongst recipients who do not have a blood-group compatible paired donor in the UKLKSS

cPRA range	Proportion
0	0.3568
[1, 10)	0.0390
[10, 20)	0.0134
[20, 30)	0.0107
[30, 40)	0.0210
[40, 50)	0.0244
[50, 60)	0.0336
[60, 70)	0.0306
[70, 80)	0.0428
[80, 85)	0.0355
[85, 90)	0.0458
90	0.0065
91	0.0126
92	0.0286
93	0.0065
94	0.0076
95	0.0157
96	0.0237
97	0.0153
98	0.0252
99	0.0966
100	0.1081

Table 13: Proportion of blood-group compatible donors marked as transplant compatible broken down by cPRA of the recipient

cPRA range	Compatibility
[0, 50)	$0.5651 - 0.3301 \times \frac{\text{cPRA}}{100}$
[50, 95)	$0.6578 - 0.6419 \times \frac{\text{cPRA}}{100}$
95	0.0583
96	0.0534
97	0.0253
98	0.0145
99	0.0152
100	0.0124

Table 14: Distribution of the proportion of blood-group compatible donors marked as transplant compatible for recipients with a cPRA of 0

Incompatibility range	Proportion of recipients
0	0.1891
(0, 0.01]	0.0683
(0.01, 0.02]	0.0774
(0.02, 0.03]	0.0387
(0.03, 0.04]	0.0205
(0.04, 0.10]	0.0547
(0.10, 0.25]	0.0592
(0.25, 0.50]	0.0911
(0.50, 0.75]	0.1412
(0.75, 1.00]	0.2597

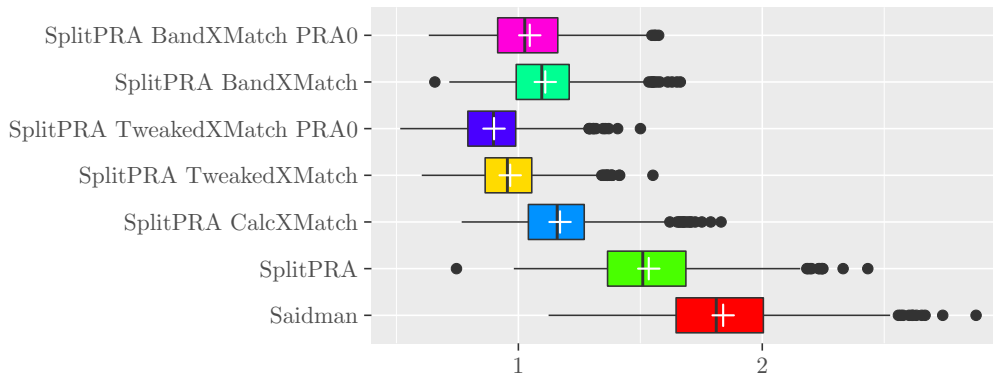


Figure 12: Number of edges as a proportion of number of edges in real-world instances

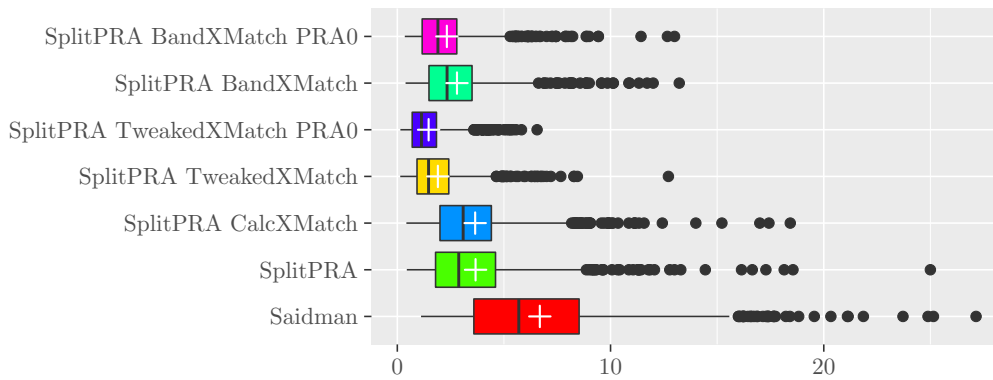


Figure 13: Number of two-cycles as a proportion of the number of two-cycles in real-world instances

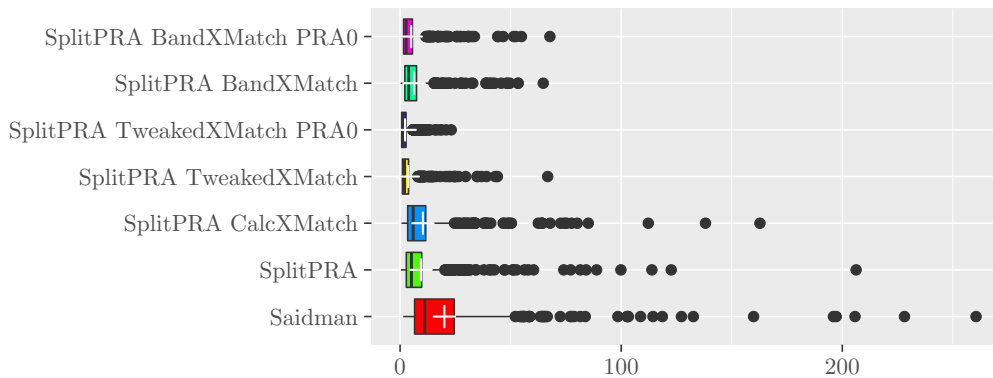


Figure 14: Number of three-cycles as a proportion of the number of three-cycles in real-world instances

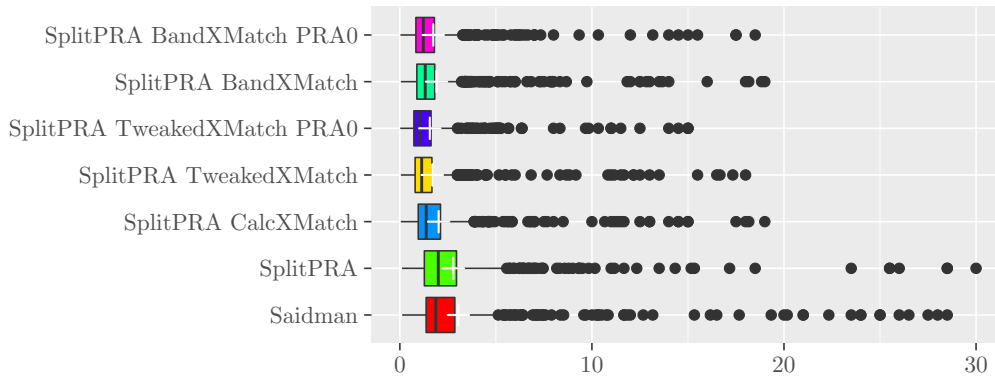


Figure 15: Number of short chains as a proportion of the number of short chains in real-world instances

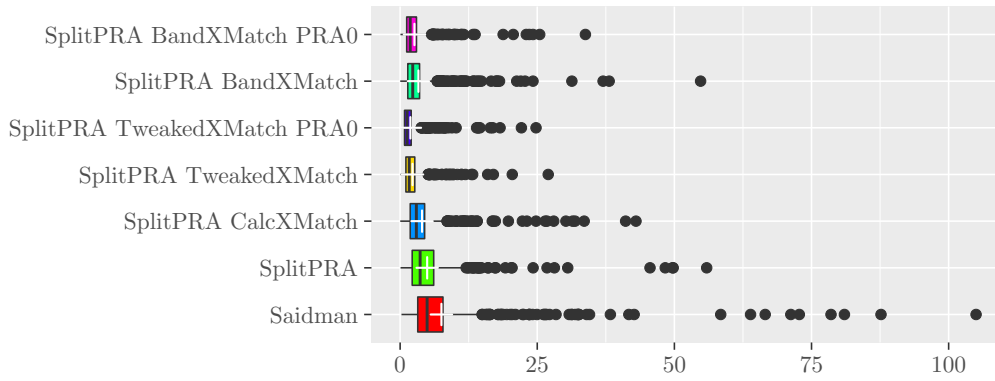


Figure 16: Number of long chains as a proportion of the number of long chains in real-world instances

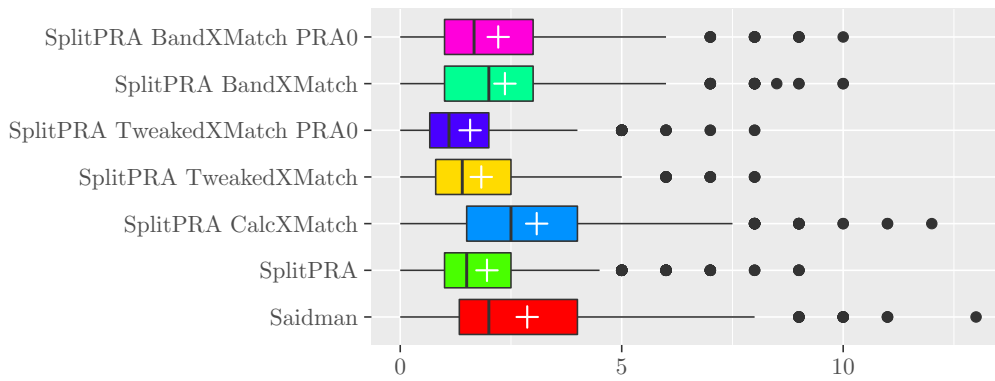


Figure 17: Number of selected two-cycles as a proportion of the number of selected two-cycles in real-world instances

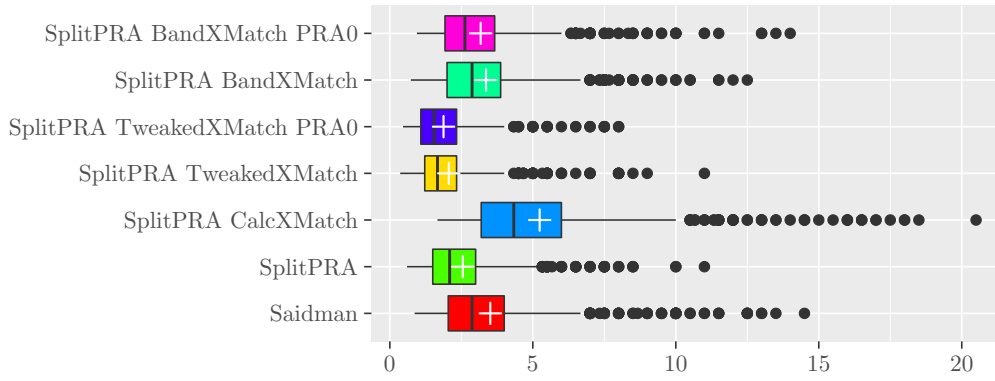


Figure 18: Number of selected three-cycles as a proportion of the number of selected three-cycles in real-world instances

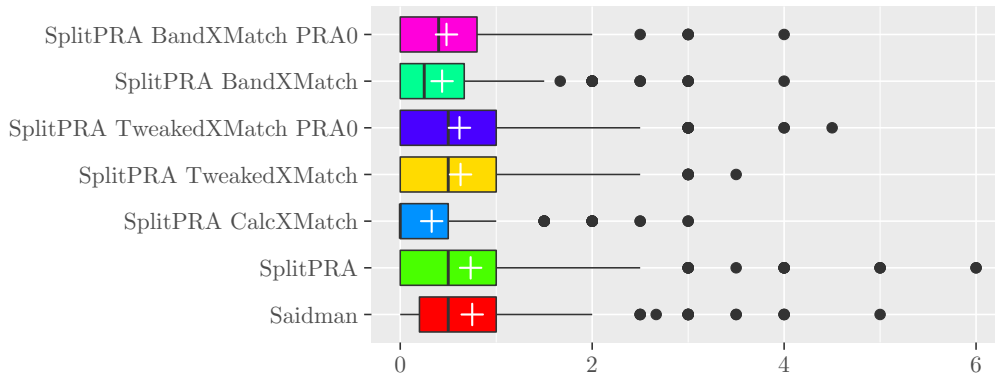


Figure 19: Number of selected short chains as a proportion of the number of selected short chains in real-world instances

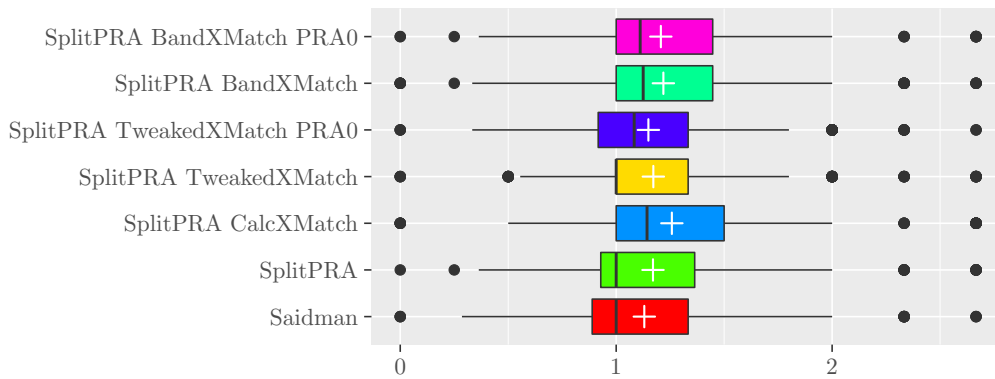


Figure 20: Number of selected long chains as a proportion of the number of selected long chains in real-world instances

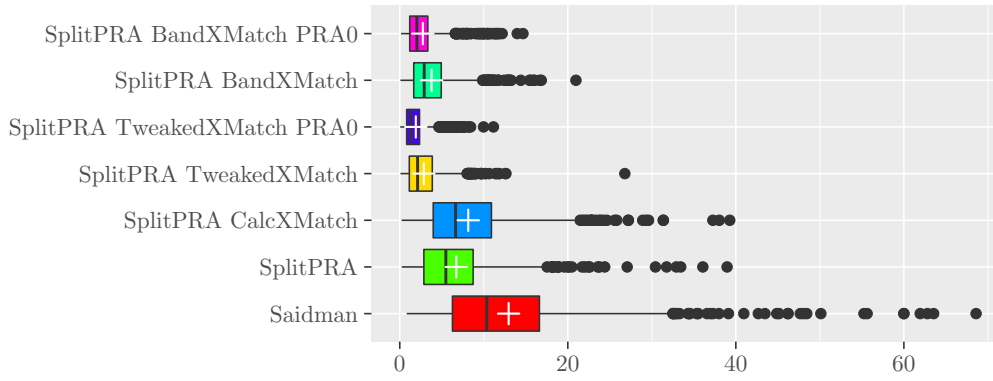


Figure 21: Time to solve IP as a proportion of the time to solve the IP for real-world instances

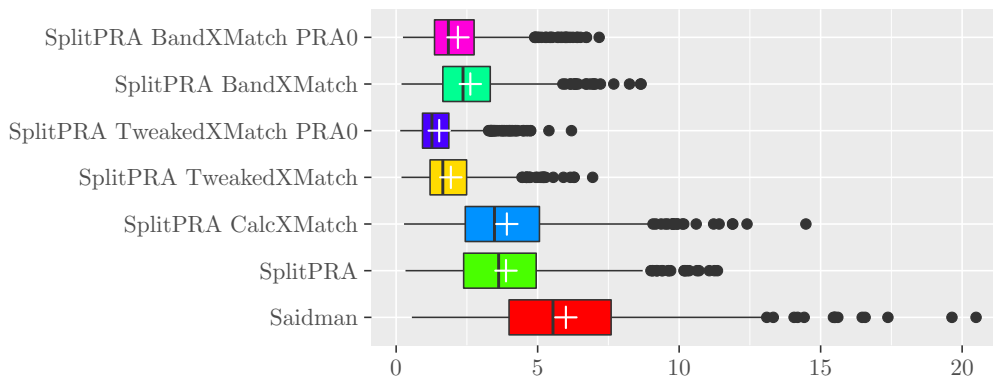


Figure 22: Time to solve total problem as a proportion of the time to solve the total problem for real-world instances